



# A Composite Structure of the Bashkir Anticlinorium: Insights from Detrital Zircons Search in Ordovician Sandstones of the Uraltau Uplift, Southern Urals

N. B. Kuznetsov<sup>1</sup>, T. V. Romanyuk<sup>2</sup>, and E. A. Belousova<sup>3</sup>

## Abstract

The Bashkir anticlinorium is an extensive outcrop of Precambrian rocks within the Southern Urals, located near the south-eastern edge of the East European Platform (EEP). The Bashkir anticlinorium is subdivided by the Zyuratkul fault into two parts: the Bashkir (western part) and Uraltau (eastern part) Uplifts. The Late Precambrian strata of the Bashkir Uplift were formed at a passive margin of the Volga-Uralian part of Baltica. In contrast, the Late Precambrian strata of the Uraltau Uplift were formed far from its present-day location. Later, the Uraltau Uplift block moved along the Zyuratkul fault to its present-day position with a large-amplitude displacement. This study presents the first results of the integrated (U-Pb age, Hf-isotope and trace-elements contents) study of detrital zircons (dZr) from the Upper Ordovician sandstones of the northern part of the Uraltau Uplift. The integrated characteristics of the studied dZr provide new constraints for their primary sources. A comparison of obtained data with rock types, U-Pb and Hf model ages of the crystalline complexes of the of Volga-Uralia basement, as well as characteristics of dZr from Late

Precambrian strata of the Bashkir Uplift and Kazakhstan have revealed that the Upper Ordovician sandstones of the northern part of the Uraltau Uplift contain dZr “alien” to crystalline complexes of Volga-Uralia, Kazakhstan, and Late Precambrian strata of the Bashkir Uplift. The sources of these “alien” dZr were other crustal blocks. A very high similarity of the age spectra of dZr from the Upper Ordovician sandstones, which overlain the Late Precambrian rocks units of the Uraltau and Bashkir Uplifts allows concluding that the spatial conjunction of the Bashkir and Uraltau Uplifts had occurred before the Late Ordovician time. Post-Upper Ordovician sedimentary complexes of the Bashkir and Uraltau Uplifts were sourced from identical feeding provinces in the same sedimentary basin, sealing its composite pre-Upper Ordovician heterogeneous basement.

## Keywords

Southern Urals • Bashkir anticlinorium • Bashkir and Uraltau Uplifts • Ordovician • Detrital zircons • U-Pb age • Hf systematic • Trace-elements • Provenance • Sources

N. B. Kuznetsov  
Geological Institute, Russian Academy of Sciences, Pygevsy 7,  
Moscow, 119017, Russian Federation

N. B. Kuznetsov (✉)  
Institute of the Earth's Crust, Siberian Branch, Russian Academy  
of Sciences, Lermontova St. 128, Irkutsk, 664033, Russian  
Federation

N. B. Kuznetsov · E. A. Belousova  
Australian Research Council Centre of Excellence for Core to  
Crust Fluid Systems/GEMOC, Macquarie University, Sydney,  
NSW 2019, Australia

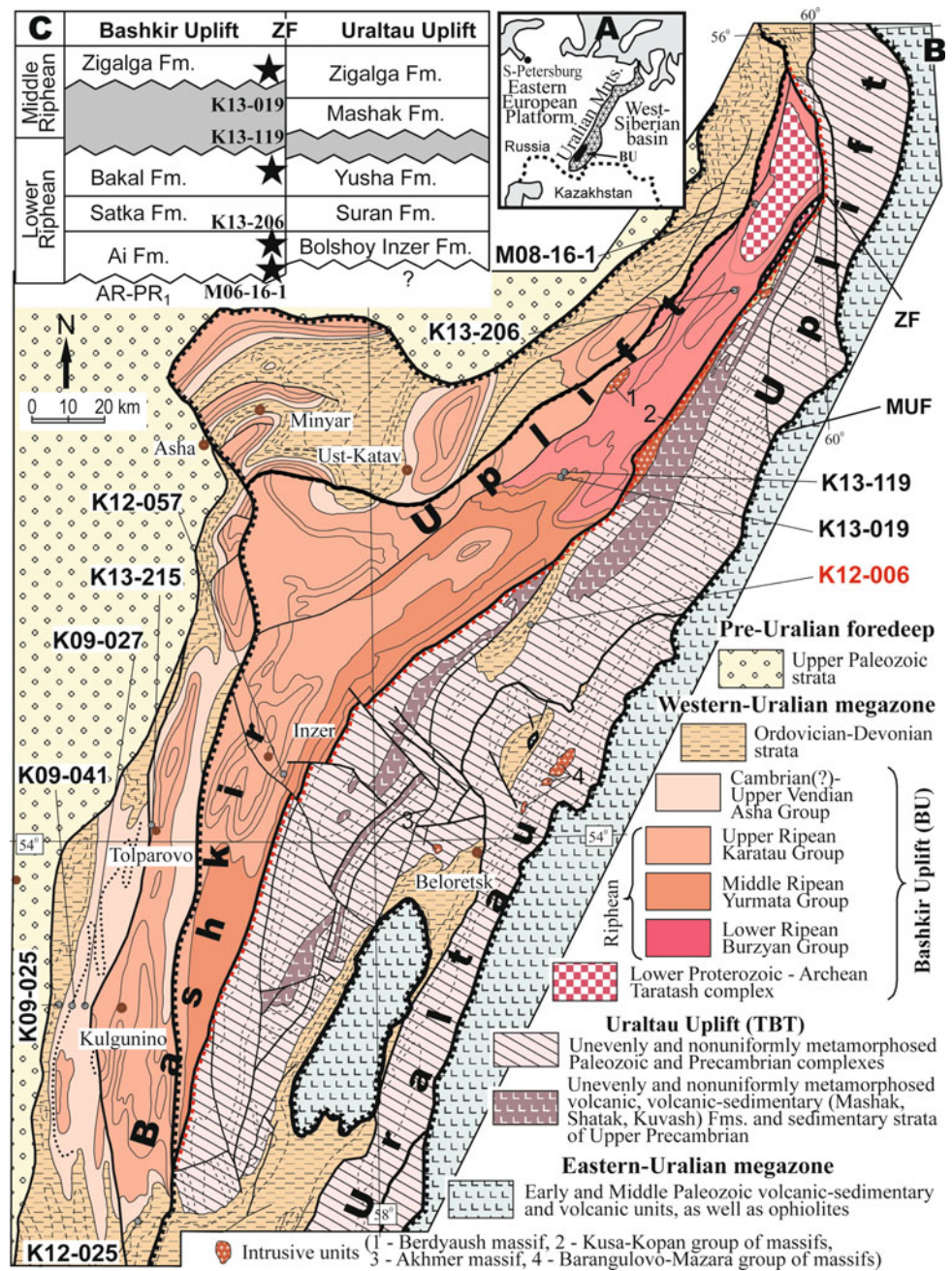
N. B. Kuznetsov  
Peoples' Friendship University of Russia (RUDN University), 6  
Miklukho-Maklaya St, Moscow, 117198, Russian Federation

T. V. Romanyuk  
Schmidt Institute of Physics of the Earth, Russian Academy of  
Science, B. Gruzinskaya 10, Moscow, 123242, Russian Federation

## 1 Introduction and Geological Settings

The Bashkir anticlinorium (BA) is located in the west of the Southern Urals (Fig. 1a). The BA is an extensive outcrop of Precambrian rocks, traditionally interpreted as a relic of a Late Precambrian passive margin of Baltica (Precambrian basement of the East European Platform) and its Early Precambrian basement (Puchkov 2010), or a relic of an inland rift-like basin, transformed at the beginning of the Paleozoic into a passive margin of Baltica (Ivanov 1998). The BA is divided into two parts by the Zyuratkul fault: Bashkir Uplift and the northern Uraltau Uplift (Figs. 1b, c).

**Fig. 1** Scheme of the geological structure of the northern part of the Western-Uralian megazone of the Southern Urals (the Bashkir anticlinorium) and the positions of the samples discussed in the text (B). Compiled using data from V.I. Kozlov (small-scale geological map, Ufa sheet), as well as authors' own materials. Faults: ZF = Zyuratkul, MUF = Main Uralian. Insert in the upper left corner: stratigraphic charts of the Bashkir and Uraltau Uplifts for Lower and Middle Riphean (C). A Index scheme



To the west of the Zyuratkul fault within the Bashkir Uplift, the Upper Precambrian Formations occur and did not experience Pre-Ordovician deformations and metamorphism (Puchkov 2010). Their lower part is composed of predominantly sedimentary (including the bottom level of the Early Riphean) non-metamorphosed rocks interpreted as a strato-typical Riphean section (Stratotype 1983; Ivanov 1998; Maslov 2004; Puchkov 2010). The upper part is composed of terrigenous formations of the Upper Vendian Asha Group (Maslov 2004; Puchkov 2010) or Upper Vendian-Cambrian in age (Kuznetsov and Shazillo 2011). Late Precambrian Formations that are unevenly

metamorphosed and experienced Pre-Ordovician deformations (Golionko and Artemova 2016; Puchkov 2010) are widespread eastward the Zyuratkul fault within the northern Uraltau Uplift (Uraltau Uplift hereafter). Middle Riphean volcanic and intrusive rocks (Mashak, Shatak, and Kuvash Formations) are widely represented here (Ivanov 1998; Maslov 2004; Puchkov 2010).

In the western and south-western Bashkir Uplift, the Upper Precambrian Formations are covered by the Paleozoic strata, the section of which begins with low-thickness Upper Emsian quartzous sandstones (Takaty Formation) (Kuznetsov et al. 2014a, b; Puchkov 2010). At the same time, in the

southern Bashkir Uplift and within the Uraltau Uplift, the Paleozoic section begins with a thin-thickness of Upper Ordovician quartzous sandstones (Kuznetsov et al. 2016; Puchkov 2010). The oldest sedimentary units overlying the Asha Group are Lower Devonian in age (Takaty Formation) in the western part of the Bashkir Uplift and Middle Ordovician age in the southern one. The most striking difference between the Paleozoic Formations that overlay the Upper Precambrian complexes within the Bashkir and Uraltau Uplifts is the nature of parallel and angular unconformities between these rocks and the underlying formations.

Differences in the structure of the Precambrian Formations of the western and eastern parts of the BA (see Fig. 1C) made it possible to suggest its composite structure (Kuznetsov 2009). In accordance with this, the Bashkir Uplift is a relic of a Late Precambrian passive margin of Baltica (Kuznetsov et al. 2013; Romanyuk et al. 2013), and the Uraltau Uplift is a relic of an alien structure in relation to the contiguous part of Baltica. The Uraltau Uplift block moved along the Zyuratkul fault to its present-day position with a large-amplitude dextral displacement (Kuznetsov 2009).

To develop and to test the idea of a composite structure of the BA (i.e. to unravel the ultimate origin and nature of the Uraltau Uplift block and details of its evolution, as well as to constrain the time of conjugation of the Bashkir and Uraltau Uplifts), we have studied detrital zircons (dZr) from different stratigraphic units of the Bashkir and Uraltau Uplifts (Romanyuk et al. 2013, 2014, 2017, 2018, 2019a, b, 2000; Kuznetsov et al. 2012, 2013, 2014a, b, 2016, 2017a, b, 2018). This paper deals with the first results of the integrated detrital zircons study of the Upper Ordovician sandstones (sample K12-006), which overlap unevenly metamorphosed Late Precambrian rocks of the Uraltau Uplift with an angular unconformity. The integrated characteristics of individual detrital zircon grains aim to better identify the provenance of dZr and to try to reveal relationships of affinity or alien relationships between studied strata and those of Volga-Uralia, Kazakhstan and the Western Urals. This paper focuses on a comparison of age spectra of dZr from Ordovician sandstones of the Uraltau Uplift (sample K12-006) and age spectra of dZr from Ordovician sandstones of the Bashkir Uplift (sample K12-025), which overlap non-metamorphosed Late Precambrian rocks with a parallel unconformity.

## 2 Methodology

The study was carried out using the TerraneChron®, analytical approach (Griffin et al. 2000, 2002, 2004, 2006, 2007; Belousova et al. 2002, 2006) developed at the CCSF/GEMOC Center (Macquarie University, Sydney). The methodology integrates in situ U-Pb age, trace-element and Lu-Hf-isotope analyses on zircons. Such an integrated

approach makes it more reliable to identify the source rocks of detrital zircons and to reconstruct the evolution of the supplying provinces than can be done based on U-Pb ages of detrital zircons only (Veevers et al. 2005, 2006; Belousova et al. 2015; Romanyuk et al. 2018; Kuznetsov et al. 2018, 2019). The study of dZr was carried out using LA-ICP-MS technique, a description of which and detailed methodology are given in previous publications (Griffin et al. 2000; Jackson et al. 2004).

U-Pb ages with discordance  $D: 10\% > D > -5\%$  are used to plot the histograms and probability density plots (PDP) of the ages (Ludwig 2012; Vermeesch 2012, 2018). For zircons with age over 1 Ga, the used age is calculated based on  $^{206}\text{Pb}/^{207}\text{Pb}$  ratio, for zircons with age younger than 1 Ga,  $^{206}\text{Pb}/^{238}\text{U}$  ratio was used.

Attempts to determine such characteristics of individual zircon grains as indicators of magmatic, metamorphic or hydrothermal (sometimes called «metasomatic») nature of a crystal (or even separate its core/rim), a forecast of the type of parental rocks of zircon, assessment of crystallization temperatures, zoning, etc., by the morphology of the crystal and metamict zones features in it, optical, CL-and BSE-images, contents of trace and REE for zircon, the composition of gas/fluid and inherited inclusions and other data, have a very long history (Heaman et al. 1990; Hoskin et al. 2000; Hoskin and Ireland 2000; Griffin et al. 2000, 2004; Liu et al. 2001; Belousova et al. 2002, 2006, 2010, 2015; Corfu et al. 2003; Hoskin and Schaltegger 2003; Liu and Xu 2004; Watson et al. 2006; Hawkesworth and Kemp 2006; Harrison et al. 2007; Grimes et al. 2007, 2015; Ferry and Watson 2007; Fedotova et al. 2008; Fu et al. 2008; Skublov et al. 2012; Fornelli et al. 2014; Chapman et al. 2016 and many others). But unlike the study of U-Pb and Lu-Hf isotopic systems of zircons, where there have been developed common adopted technologies, the interpretation of concentrations of trace and REE elements in zircons has not been yet developed up to a generally accepted technology.

There were many attempts to develop some criteria to distinguish magmatic, metamorphic and hydrothermal zircons (e.g. Rubin et al. 1989, 1993; Corfu and Davis 1991; Claoue-Long et al. 1990; Kerrich and King 1993; Ramezani et al. 2000; Hu et al. 2004; Hoskin 2005; Schaltegger et al. 2005; Pettke et al. 2005; Kebede et al. 2007; Pelleter et al. 2007; Fu et al. 2009; Rubatto 2017 and many others). For example, Hoskin and Schaltegger (2003) had tried to summarize textural and compositional characteristics of hydrothermal zircons, but they had to conclude that the characteristics are not definitive. The hydrothermal zircons may be zoned or unzoned on cathodoluminescence images (CLI); spongy in texture; anhedral or faceted in morphology; and either high or low in common-Pb. By now, there are no doubtless criteria to distinguish between metamorphic and magmatic zircons.

Nevertheless, it has been reliably established that certain statistical trends and appreciable differences in the trace-elements contents are recorded in zircons from certain types of rocks and different origins (Hoskin and Ireland 2000; Hoskin 2005; Belousova et al. 2002, 2006, 2015; Schulz et al. 2006; Fedotova et al. 2008; Kaczmarek et al. 2008; Kostitsyn et al. 2015; Fershtater et al. 2012; Grimes et al. 2015, and others). Thus, in general, Rare Earth Elements (REE) contents in zircons increase from basic rocks (gabbroids and basaltoids), in which the total content of REE is  $(5-10) \times 100$  ppm up to  $(1-2) \times 1000$  ppm, to felsic rocks (granitoids and their effusive analogs), in which the total content of REE is  $(2-5) \times 1000$  ppm. Furthermore, the REE contents in zircons from pegmatites and nepheline syenites can reach even 1–3 mass %. For such rocks as kimberlites, the typical total content of REE in zircons is usually less than 50 ppm. In zircons from carbonatites and lamproites the total REE content is larger and can increase up to 500 ppm (Belousova et al. 2002, 2015), but its average value is 100–250 ppm (Hoskin and Ireland, 2000).

An important indicator is the Th/U ratio (see the review by Kirkland et al. 2015; Rubatto 2017), which varies from 0.1 to 1 in most zircons. Low Th/U ratios are statistically considered to be characteristic of zircon crystals of metamorphic origin, unlike zircons of magmatic origin. However, there is still no consensus on the threshold Th/U value: in different works, values Th/U from 0.5 to 0.1 are established. Thus, value 0.5 in (Kirkland et al. 2015), 0.2 in (Hoskin and Schaltegger 2003), 0.1 in (Teipel et al. 2004). In general, the accumulated data (see Rubatto 2017) indicate that Th/U values from 0.5 to 0.1 are fixed in zircons of both magmatic and metamorphic origin. For example, zircon rims from the Sulu UHP mafic and felsic rocks show higher values of Th/U up to 0.4 (Zhang et al. 2009). On the other hand, zircons crystallized in granites at low temperatures are characterized by higher U contents and lower Th, which, as a result, leads to lower Th/U values in low-temperature crystals (Harrison et al. 2007). Therefore, in the diagrams, we mark the interval Th/U from 0.5 to 0.1 as «Zircons magmatic or metamorphic origin» and believe that only zircons with a ratio Th/U < 0.1 can have a metamorphic origin with a high degree of probability.

High ratios of Th/U > 1.5, together with other characteristics, are statistically inherent in zircons from mafic rocks (Heaman et al. 1990; Kaczmarek et al. 2008; Linnemann et al. 2011). It can't be ignored that in the zircons with high Th/U are sometimes formed in environments of high degrees of metamorphism (Wanless et al. 2011).

Very low U/Yb ratios are recorded for zircons from oceanic basalts NMORB (U/Yb < 0.1) (Grimes et al. 2015). Higher values U/Yb are not unique and can be inherent in a wide range of rocks. However, in general, an increase in the ratio of U/Yb and the Hf content in zircons indicate the

fractionation of their parent magmas and reflect the trends in their composition in the direction from the primitive crust towards a more enriched crust. The diagrams «U/Yb versus Hf» and «U/Yb versus Nb/Yb» are most statistically effective for distinguishing between zircons from oceanic basalts and zircons from the continental crust (Grimes et al. 2015).

Important information on zircons is carried by the REE spectra, which are represented in the form of values normalized to chondrite (we use the values for CI-chondrite from (McDonough and Sun 1995)). A monotonic increase in the content of elements from light to heavy is typical for the normalized REE spectra of zircons, which is complicated by two anomalies: positive Ce and negative Eu.

The REE spectra of zircons from granitoids are highly ordered for the heavy REEs: in the interval from Dy to Lu, the slope of the zircon spider diagrams is rather stable. Its value is characterized by the Lu/Dy (sometimes Yb/Sm or Lu/Gd) ratio, and the contents of the heaviest REEs (Yb and Lu) are used as a marker for classifications. Statistically, the zircon that is crystallized in the igneous rock has a steeper slope for heavy REEs (larger Yb/Sm values) than the crystal formed in rocks of high degrees of metamorphism (Rubatto and Hermann 2007; Rubatto 2017).

For zircons of high-temperature metamorphic origin, which are crystallized in the presence of garnet, the lower heavy REE and Y are described (Rubatto 2002; Rubatto and Hermann 2007; Fedotova et al. 2008; Skublov et al. 2012; Fornelli et al. 2014), because the garnet competes with zircon on these items. For eclogites, also a low Th concentration (no higher than 3 ppm on average) and a significant decrease in the concentrations of all REE (to 22 ppm) and particularly LREE (<2 ppm), and relatively low concentrations of Y (34 ppm), U (100 ppm), and P (41 ppm) at an elevated Hf concentration (11 400 ppm on average) have been revealed (Skublov et al. 2012).

The discriminative «(Sm/La)<sub>N</sub> versus La» and «Ce/Ce\* versus (Sm/La)<sub>N</sub>» diagrams based on distinct REE patterns from magmatic and hydrothermal zircons were presented in (Hoskin 2005). Further researches revealed that not all data points reported for zircons which are thought to be hydrothermal ones fill in the «hydrothermal» area in this discriminate diagram (Fu et al. 2009). However, the proposed in (Hoskin, 2005) signs of «uplifted» LREEs spectra (a higher content of La (La > ~ 2 ppm) and a lower (Sm/La)<sub>N</sub> ((Sm/La)<sub>N</sub> < 10)) and weak Ce/Ce\* anomaly (Ce/Ce\* < 10) are the effective indicators to suppose if not a pure hydrothermal origin of zircon, but at least a hydrothermal imprint on the zircon. Metamictic zircons also often show «uplifted» LREE spectra.

The above information was summarized in the scheme of classification shown in Fig. 2 to distinguish between a magmatic/metamorphic/hydrothermal origin of zircon. For zircons whose magmatic origin is supposed, the CART

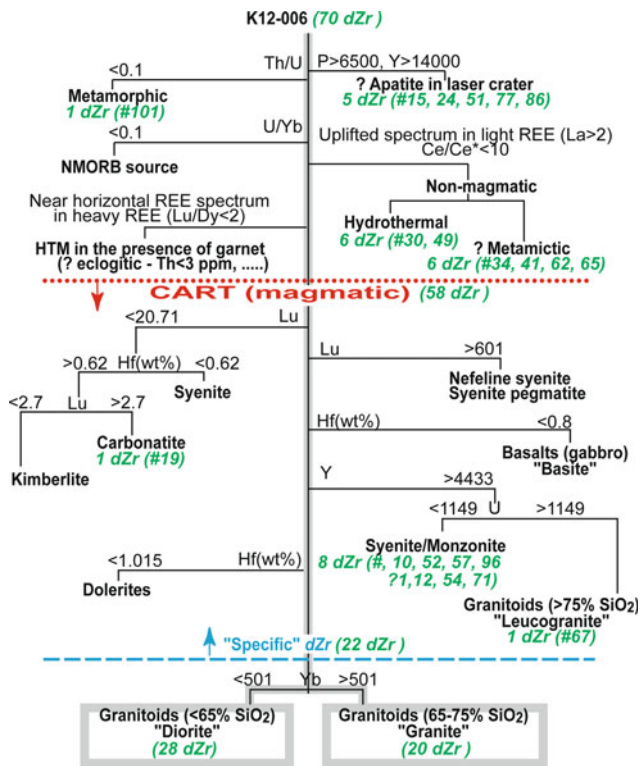


**Fig. 2** The scheme of classification of detrital zircons (dZr) from sample K12-006 based on the CART algorithm (Belousova et al. 2002); a number of dZr of each type in studied samples are marked by green bold italic letters

algorithm (Belousova et al. 2002) was applied to predict a type of parental zircon rocks. The main purpose of using the CART algorithm is the primary separation of zircons, the parental rocks for which there could be rare rock complexes («specific» zircons), from zircons from granitoids and their effusive material analogues, which are the main sources of zircon. The latter, as a result of the classification, are subdivided by the percentage of SiO<sub>2</sub> in the rock into three groups—rocks with reduced (SiO<sub>2</sub> < 65%), normal (SiO<sub>2</sub> = 65–75%) and increased (SiO<sub>2</sub> > 75%) SiO<sub>2</sub> contents. For the sake of brevity, these groups are called, respectively, «diorite», «granite» and «leucogranite» and corresponding zircons as «dioritic», «granitic», «leucogranitic».

Unlike zircons from «granites» or «diorites», which form large groups, are determined and interpreted statistically, the identification of «specific» zircons requires «manual» testing and debugging, checking the occurrence of measured trace-elements concentrations at boundary marker values for the concentrations of the elements the CART algorithm operates on. For example, a content of Y = 4433 ppm is the marker to distinguish between «granite» and «syenite/monzonite». If content Y in zircon is a little bit less than 4433 ppm, for example, Y = 4400 ppm, then this

zircon is classified as «?syenite/monzonite» and is additionally checked in other classification diagrams (Summary REE versus Ti and REE spectra). The reliability of this approach and the percentage of misclassification are discussed in Belousova et al. (2002).

### 3 Sampling Rocks; Separation, Imaging, Morphology and Analytical Results of Detrital Zircons Study

#### 3.1 Sampling Rocks, Imaging and Morphology Zircons, Measurements, Standards

Sample K12-006 (~1.5 kg) was collected from the light-yellow fine-middle-grained quartzous sandstones in the basal level of the Paleozoic section (see sample location in Fig. 1) on the south-western slope of the Yuryuzan syncline (53°36'21.15" N and 58°46'57.30" E) on the left side of the Tyulyuk spring (a right tributary of the Yuryuzan River). Approximately 300 zircon grains were separated from the sample (technology is described in Romanyuk et al. 2018), of which 202 randomly selected grains were mounted into an epoxy disk.

Zircons were studied with a microscope and in cathode rays and backscattered electrons (BSE). All grains are rounded, mostly small (<100 μm). Almost all dZr contain inherited inclusions, metamict zones, and in some cases are broken by cracks. These are indications that zircons participated in magmatic/metamorphic processing (Corfu et al. 2003). For dating, we selected grains in which we managed to map out areas (Ø ≤ 40 μm) using CLI without obvious metamictization, violations, inclusions and cracks.

At the first stage, the simultaneous measurement of the U-Pb-isotope system and trace-elements contents of dZr was executed, at the second stage, a separated study of the Lu-Hf-isotope system of the selected dZr were executed. Measurements of the parameters of the U-Pb-isotope system in zircons were carried out with the Red-JG-1 zircon standard for calibration (Jackson et al. 2004; Elhlou et al. 2006), and Mud-Tank and 91,500 as measured zircons for monitoring. During the measurements, the mean ages were Mud-Tank = 737 ± 5 Ma (n = 7) and 91,500 = 1059 ± 8 Ma (n = 7), which agrees with the ages of these standards (Wienedbeck et al. 1995, 2004; Jackson et al. 2004; Black et al. 2004; Yuan et al. 2008; Horstwood et al. 2016).

Measurements of the Lu-Hf-isotope system were monitored by Mud-Tank and Temora II zircon standards. During the measurements, the average ratio of <sup>176</sup>Hf/<sup>177</sup>Hf was 0.282551 ± 0.0000086 (n = 4) for Mud-Tank and 0.282619 ± 0.000025 (n = 4) for Temora II, which is in

agreement with the values for these zircon standards (Jackson et al. 2004; Yuan et al. 2008). Measurement of the content of trace elements in dZr was carried out for 22 elements, the NIST standard was used for external control. Data processing was performed using the commercial program “GLITTER” (Griffin et al. 2008) and the programs (Ludwig 2012; Vermeesch 2012, 2018) available in the public free access.

### 3.2 U–Pb Age Results

A total of 70 analyses were performed. For 12 grains, a large analytical error ( $>50$  Ma, #51) or strongly discordant analyses (#17, 24, 51, 77 and 41) have been obtained (Fig. 3). These analyses were excluded from consideration. The remaining 58 analyses were used to plot the age histogram and the PDP (Fig. 4a). The youngest age is  $530 \pm 4$  Ma ( $D = 6.8\%$ , #30) and the oldest is  $2885 \pm 31$  Ma ( $D = -0.3\%$ , #50).

### 3.3 Zircon Trace-Element Content and Parental Rock Type Classification

When studying the trace-elements content (Figs. 4b, 5, 6, 7, 8, 9, 10, 11 and 12), the La content was not determined for

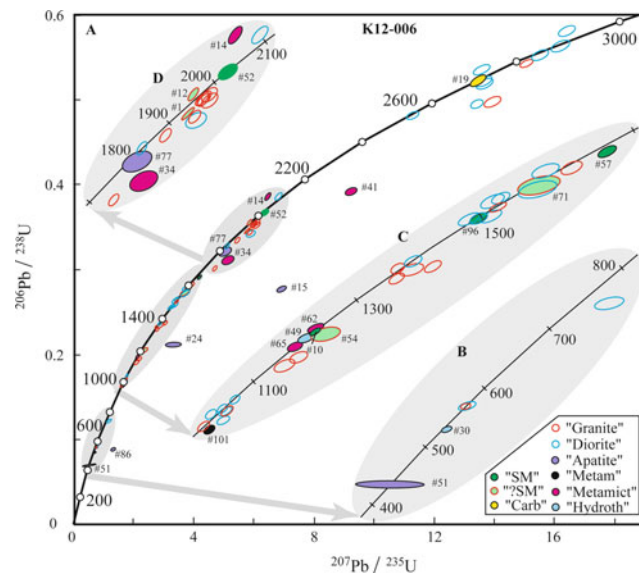


**Fig. 3** Results of the U–Pb dating of detrital zircons from the K12-006 sample. A—Concordia and ellipses (some with analysis numbers), showing a 68.3% confidence interval for measurements. B, C and D (at the grey background)—the enlarged fragments of Concordia. Classification of the zircons (see Table 1 and Fig. 2): “SM” = «syenite/monzonite», “?SM” = «granite», but probably «syenite/monzonite», “Carb” = «carbonatite», “Metamictic” = metamictic zircon, “Hydroth” = hydrothermal zircon, “Apatite” = apatite inclusion in the LA sampling, “Metam” = metamorphic zircon

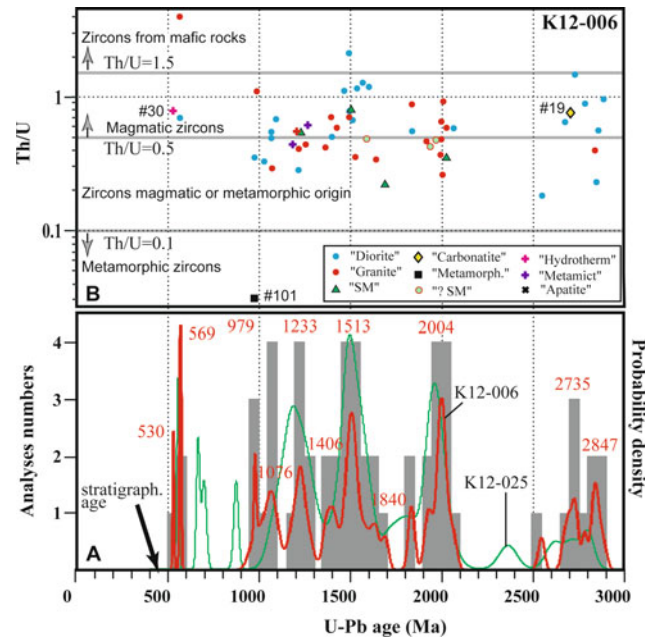


**Fig. 4** Histograms and the Probability Density Plot (PDP) of U–Pb ages («conditioned» analyses only) (A) and Th/U values (B) of detrital zircons from sample K12-006. PDP (green line) for sample K12-025 (Ordovician, Bashkir Uplift, Kuznetsov et al. 2016) is added in (A)

grains # 19, 28, 43, 44, 45, 46, 56, 84, 95 and 101 (the content is below the detection limit). Further, for calculating Ce anomalies, the La content for these zircons was adopted at 0.01 ppm. Five grains have yielded anomaly high P and Y contents (Table 1), which may suggest an apatite inclusion in the LA crater. They also show very high contents of total REE and Ti (Fig. 7). They are marked as «apatite» in Table 1.

Zircon #101 showed very low  $\text{Th/U} = 0.03$  (Fig. 4b) and it was classified as «metamorphic». It also differs from other zircons in a high content of Hf (Fig. 9) and steep REE spectra in heavy REE (Figs. 6 and 8).

Seven zircons (#14, 30, 34, 41, 49, 62 and 65) showed elevated La content of more than 2 ppm and weak Ce/Ce\* anomalies less than 10. Their data points on discriminant diagrams in Fig. 5 fall in a field far besides «Magmatic zircons fields», so they were classified as «non-magmatic» zircons. Two zircons (#30 and 49) from «non-magmatic» zircons fit well to fields of «Hydrothermal zircons» in discriminant diagrams of Fig. 5 and were classified as «Hydrothermal zircons». The rest «non-magmatic» zircons are marked as «Metamictic». There were revealed no zircons with flat REE spectra in heavy REE (Figs. 6 and 8) that would suggest their «HTM-Gr» origin, neither zircons with the signature of NMORB (Fig. 12).

For the 58 detrital zircons having the most probable magmatic origin, the CART classification (Fig. 2) indicates that the parental rocks were most likely «granites» (24) and

**Table 1** Some characteristics of the studied zircons with specific trace-element contents and results of their classification

#	Analysis #	Th/U	P (ppm)	Y (ppm)	La (ppm)	Yb (ppm)	Lu (ppm)	U (ppm)	Total REE (ppm)	Lu <sub>Cl</sub> /Dy <sub>Cl</sub>	Hf %	U-Pb Age ± 1σ (Ma)	D%	ε <sub>Hf</sub> (Epsilon Hf)	T <sub>DM</sub> <sup>C</sup> (Ga)	Classification
1	1	0.43	1826	4353	0.38	1245	219	464	2835	5.42	2.13	1968 ± 18	2.7	-4.2 ± 0.7	2.9	?SM
2	10	0.52	525	5249	0.28	1344	227	672	3260	4.25	1.47	1230 ± 17	0.8	5.5 ± 0.7	1.7	SM
3	12	0.42	1820	4334	0.16	1336	239	367	2837	6.60	2.09	1937 ± 15	-2.0	0.4 ± 0.6	2.6	?SM
4	14	0.89	165	1930	2.66	446	89	154	1063	3.27	1.36	1969 ± 19	-8.8			Metc
5	15	0.55	12,698	28,252	47.88	1721	230	1184	11,035	7.52	1.05	2651 ± 22	45.2			Apatite
6	19	0.741	271	429	<0.008	116	20.5	98	287	4.82	1.90	2703 ± 17	-0.8	-2.5 ± 0.5	3.3	Carbon
7	24	0.465	20,163	36,674	9.23	5851	798	1018	20,244	1.66	2.11	*1842 ± 83	35.7			Apatite
8	30	0.784	3080	1768	68.32	587	107	685	1626	6.72	1.71	530 ± 4	6.8	7.3 ± 0.5	1.1	Hydroth
9	34	0.497	789	1647	2	431	77	576	1212	3.53	1.90	1941 ± 47	11.0			Metc
10	41	0.65	1349	4202	2.48	636	105	741	2701	1.44	1.96	*2556 ± 22	19.1			Metc
11	49	0.546	3302	4402	45.52	1153	196	230	3127	4.13	1.60	1269 ± 31	4.6			Hydroth
12	51	0.372	12,081	16,806	74.72	3322	509	3106	10,750	2.50	1.56	435 ± 4	-2.4			Apatite
13	52	0.35	537	5058	0.26	1317	219	785	3194	4.33	1.89	2027 ± 26	0.03	4.2 ± 0.6	2.4	SM
14	54	0.474	1568	4207	0.95	972	163	806	2800	3.27	1.90	1292 ± 52	6.4			?SM
15	57	0.221	2567	5241	0.84	2365	439	499	4384	11.27	2.21	1692 ± 18	2.9	-1.1 ± 1.0	2.5	SM
16	62	0.555	261	1725	2.08	401	69	112	1127	3.39	1.44	1208 ± 30	0.1	5.5 ± 0.4	1.7	Metc
17	65	0.44	600	3245	2.97	840	145	414	2050	4.53	1.96	1185 ± 29	-0.1			Metc
18	71	0.48	302	3940	0.15	1064	163	483	2559	3.93	1.65	1593 ± 44	1.4			?SM
19	77	0.124	6947	15,024	7.46	2220	368	2659	8302	1.67	2.70	*1850 ± 50	3.0			Apatite
20	86	2.034	10,818	14,468	111.37	3082	520	2537	11,678	2.39	1.31	549 ± 71	71.7			Apatite
21	96	0.81	611	8632	0.20	2323	394	926	5392	4.87	1.53	1506 ± 24	0.9	3.2 ± 0.5	2.1	SM
22	101	0.022	145	1151	<0.012	668	159	700	1140	22.95	2.82	978 ± 7	7.0	19.6 ± 0.7	0.5	Metamor

Notes: D = 100% \* (age<sup>206Pb/238U</sup>/age<sup>207Pb/206Pb</sup>) - 1). Correction for non-radiogenic lead was executed in according to (Andersen 2002). The model ages of the T<sub>DM</sub> mantle and the crustal substrate T<sub>DM</sub><sup>C</sup> (two-stage model) were estimated. T<sub>DM</sub><sup>C</sup> assumes that zircon parental magma originated from an average continental crust (<sup>176</sup>Lu/<sup>177</sup>Hf for the averaged crust = 0.015) that was produced from the depleted mantle (Griffin et al., 2000, 2004, 2006; Belousova et al., 2006, 2010; Liu et al., 2013). The decay-constant λ for <sup>176</sup>Lu was adopted as λ<sup>176</sup>Lu = 1.867 × 10<sup>-11</sup> yr<sup>-1</sup> (Scherer et al., 2001). The current ratios in chondrite (<sup>176</sup>Hf/<sup>177</sup>Hf)<sub>CH</sub> = 0.282785 ± 0.000011 and (<sup>176</sup>Lu/<sup>177</sup>Hf)<sub>CH</sub> = 0.0336 ± 0.0001 were taken from (Bouvier et al., 2008), in the depleted mantle (<sup>176</sup>Hf/<sup>177</sup>Hf)<sub>DM</sub> = 0.28325 and (<sup>176</sup>Lu/<sup>177</sup>Hf)<sub>DM</sub> = 0.0384 from (Griffin et al., 2000) T<sub>DM</sub> = 1/λ × ln{1 + ((<sup>176</sup>Hf/<sup>177</sup>Hf)<sub>Z</sub> - (<sup>176</sup>Hf/<sup>177</sup>Hf)<sub>DM</sub>)/((<sup>176</sup>Lu/<sup>177</sup>Hf)<sub>Z</sub> - (<sup>176</sup>Lu/<sup>177</sup>Hf)<sub>DM</sub>)}, T<sub>DM</sub><sup>C</sup> = T<sub>DM</sub> - (T<sub>DM</sub> - t) × ((F<sub>C</sub> - F<sub>Z</sub>)/(F<sub>C</sub> - F<sub>DM</sub>)), F<sub>C,Z,DM</sub> = {((<sup>176</sup>Lu/<sup>177</sup>Hf)<sub>Z</sub>)/((<sup>176</sup>Lu/<sup>177</sup>Hf)<sub>CH</sub>)}

Classification: SM = «granite», but probably «syenite/monzonite», ?SM = «granite», but probably «syenite/monzonite», because a small deviation down from CART-criteria (Y = 4433 ppm); Carbon = «Carbonatite»; Metamor = metamorphic zircon (Th/U < 0.1); «Hydroth» = probable hydrothermal origin, «Metc» = probable metamorphic alteration of zircon; Apatite = probable apatite inclusion in the studied zircon due to high P (>6500 ppm) and Y (>14,000 ppm); \* near U-Pb Age—correction of age for common-Pb is > 20 Ma

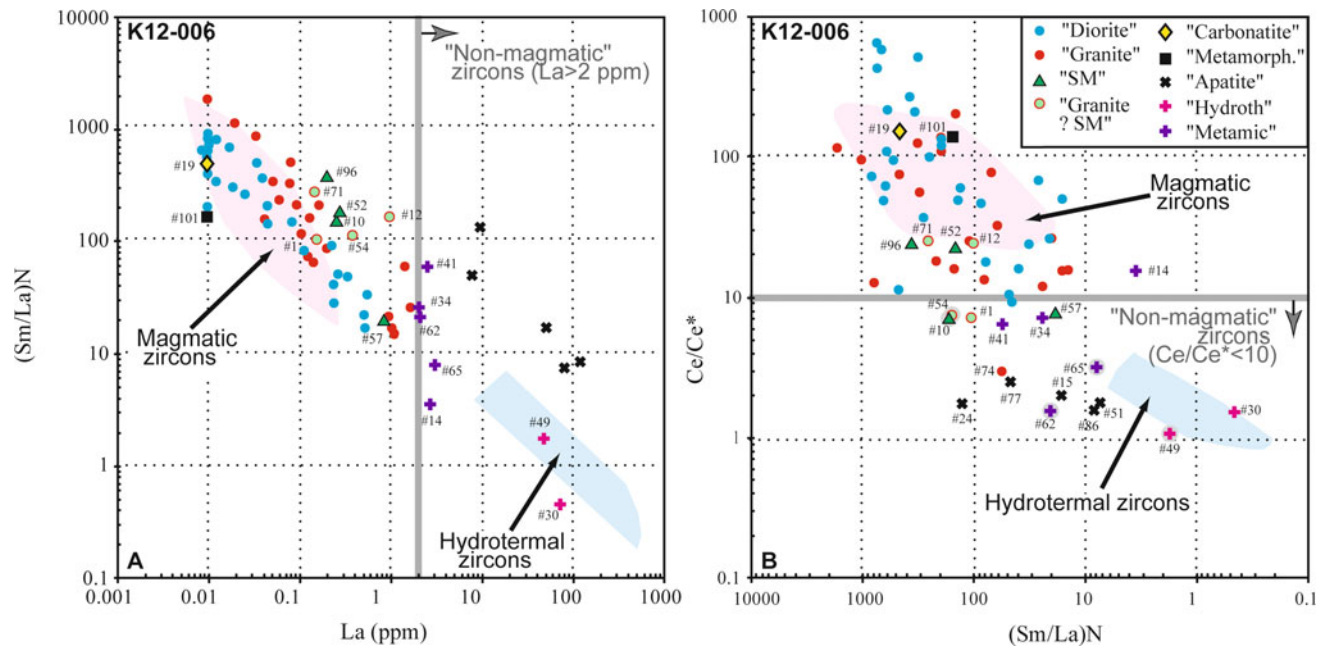


**Fig. 5** Discriminant diagrams of  $\langle (\text{Sm}/\text{La})_N$  versus La (ppm)  $\rangle$  (A) and  $\langle \text{Ce}/\text{Ce}^*$  versus  $(\text{Sm}/\text{La})_N$   $\rangle$  (B) for studied zircons from sample K12-006. The two outlined pink and blue areas are defined by magmatic and «hydrothermal» zircons from the Boggy Plain Zoned Pluton (Hoskin 2005)

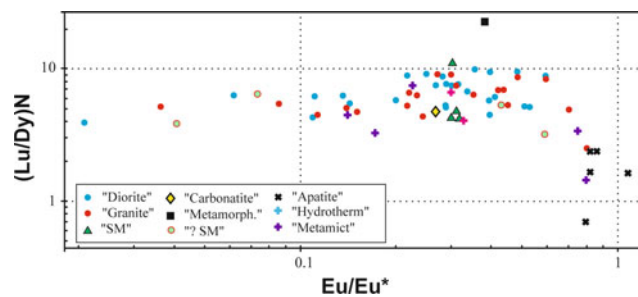


**Fig. 6**  $\langle (\text{Lu}/\text{Dy})_N$  versus  $\text{Eu}/\text{Eu}^*$   $\rangle$  diagram for detrital zircons from sample K12-006

«diorites» (28) for the majority of zircons. In the classification diagrams, zircons from «diorites» are characterized by higher contents of Yb, Y, total REE and heavy REE compared to zircons from «granites». As a specific, the parental rocks were assigned «carbonatite» (1) and «syenites/monzonite» (4). Characteristics for four «granitic» zircons are very close to the thresholds values between «granites» and «syenites/monzonite», so they were marked as «?syenites/monzonite».

«Carbonatitic» zircon (#19) is clearly distinguished from other zircons by low total REE (Fig. 7), low Lu (Fig. 8) and Y (Fig. 9) contents. In contrast, «syenites/monzonite» zircons have the upper total REE (Fig. 7) and Y (Fig. 9) contents. No other clear signs of zircons were noted in other discriminant diagrams such as «Ta versus Nb» (Fig. 10) and others.

### 3.4 Hf Isotope Analysis of the Detrital Zircons

For  $d\text{Zr}$ , the size of which allowed a second crater of  $40 \mu\text{m}$  size and the U-Pb age estimates yielded an acceptable concordance, the Lu-Hf isotope zircon system was also studied (Fig. 13a). Zircon #101 («metamorphic», age of 978 Ma) has yielded a very high value of  $\varepsilon_{\text{Hf}} = 19.6 \pm 0.7$ . This value is essential higher  $\varepsilon_{\text{Hf}}$  of the depleted mantle of this age and  $T_{\text{DM}}^{\text{C}} = 0.6 \text{ Ga}$  which is less than the U-Pb age of the zircon. Together with other atypical characteristics of this zircon (very steep spectra in Heavy REE (Figs. 6 and 8)

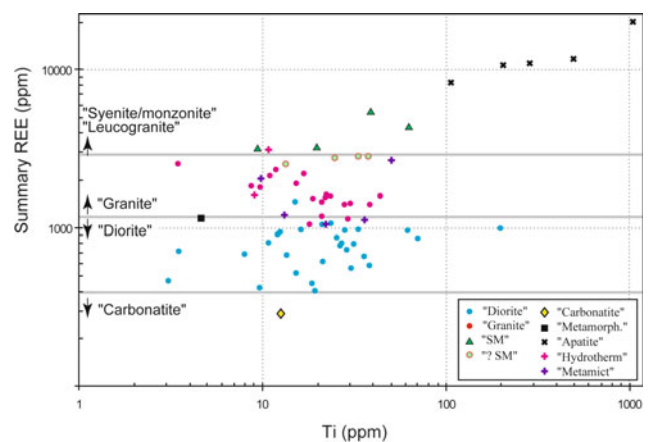
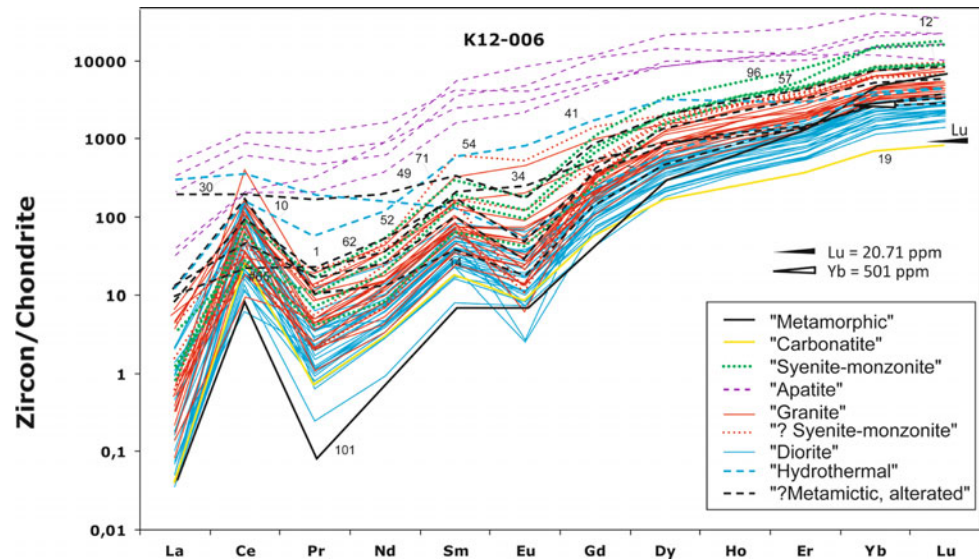


**Fig. 7**  $\langle \text{Sum or total REE versus Ti} \rangle$  diagram for detrital zircons from sample K12-006

**Fig. 8** Chondrite-normalized spider-diagram of REE contents in detrital zircons from sample K12-006



and very high contents of Hf (Fig. 9)), all these supposes a complicated history or/and structure of this zircon. Although CLI of this zircon did not show any inclusion within the LA crater area, it is possible that a deeply located inclusion does get in the LA sampling material, so we prevent giving any meaningful interpretation to this zircon. One more zircon has yielded strongly positive  $\varepsilon_{\text{Hf}} = 13.7 \pm 3.0$  (#47) which is close to  $\varepsilon_{\text{Hf}}$  of a depleted mantle of this age. All others  $\varepsilon_{\text{Hf}}$  are within interval (-9.0 + 8.8). No zircons with strongly negative  $\varepsilon_{\text{Hf}}$  were revealed that would yield unreasonably very old  $T_{\text{DM}}^{\text{C}}$ , and obtained estimates  $T_{\text{DM}}^{\text{C}}$  vary in the interval 1.1–3.4 Ga.

#### 4 Discussion and Interpretation of Obtained Analytical Data

The integrated isotope-geochemical characteristics of the studied dZr were compared with known data on the composition, age and model ages of the crystalline complexes of the Western Urals and Volga-Uralia, as well as with characteristics of dZr from Riphean strata of the Northern Kazakhstan (Fig. 13) and Bashkir Uplift (Fig. 14).

All data points of Archean dZr (10 zircons) from sample K12-006 form a compact area in «Diagrams  $\varepsilon_{\text{Hf}}$ » (Fig. 13a) within values U-Pb ages 2.55–2.90 Ga and  $\varepsilon_{\text{Hf}}$  -2.5 to +2.5. This compact area does not match the known fields of the Archean complexes Volga-Uralia: the «Tashlyar», «Aktanysh», «Bak-2» and «Kolyvan enderbites». The only 3 «dioritic» points are located back to back to the «Bak-1» field and the «carbonatitic» point fits well to the «Bak-1» field. The «Bak-1» field characterizes the quartz diorite of the Bakal block. Note that the predicted type of parent rocks of most of the Archean dZr is «diorites», which coincides

with the type of rocks of the Bakal block. However, we think that available data does not allow us to identify quartz diorites of the Bakal block as a local source. If the basement of the Volga-Uralia has been the primary source of Archean zircons for Upper Ordovician sandstones of Uraltau Uplift, we would have seen a much wider variety of ages and Hf isotope signs of dZr, including dZr with ages >2.9 Ga and dZr with Hf isotopic signs of the oldest continental crust ( $T_{\text{DM}}^{\text{C}} > 3.5$  Ga) that typical for the Volgo-Uralian basement. Note that such zircons have been found in sandstones of all Riphean stratigraphic levels in the Bashkir Uplift (Fig. 14). So, the obtained data do not allow us to allocate the basement of the Volga-Uralia and Riphean strata of the Western Urals as the most probable primary source of Archean dZr from sample K12-006. It is highly likely that it was a Neoproterozoic block beyond the Volga-Uralia, composed of mostly juvenile rocks of intermediate to mafic in composition and including some alkaline rocks.

The data points of the Paleoproterozoic dZr form area in «Diagrams  $\varepsilon_{\text{Hf}}$ » (Fig. 13a) with a range of the values of  $\varepsilon_{\text{Hf}}$  from the maximum positive («DM» composition) to substantially negative values ( $\varepsilon_{\text{Hf}} = -10$ ) corresponding to the Hf-model ages of the magma-generating substrate with  $T_{\text{DM}}^{\text{C}} = 3.0$  Ga. Such arrays are a sign of mixing juvenile and isotope-mature materials, which can occur in long-acting volcanic arcs on continental margins or in collision orogeny tectonic settings. A large body of geochronological data on crystalline rocks occurring in Paleoproterozoic orogens has been accumulated (Zhang et al. 2012). Most of these orogens are composed of complexes with ages <2.0 Ga. Ages of 2.1–2.0 Ga have been obtained within the EEP only for the Volga-Sarmatian orogen (Bibikova et al., 2009; Terentiev and Santosh, 2016; Terentiev et al., 2016a, b, 2017, 2018) and the Taratash Orogen (Sindern et al. 2005; Tevelev et al.

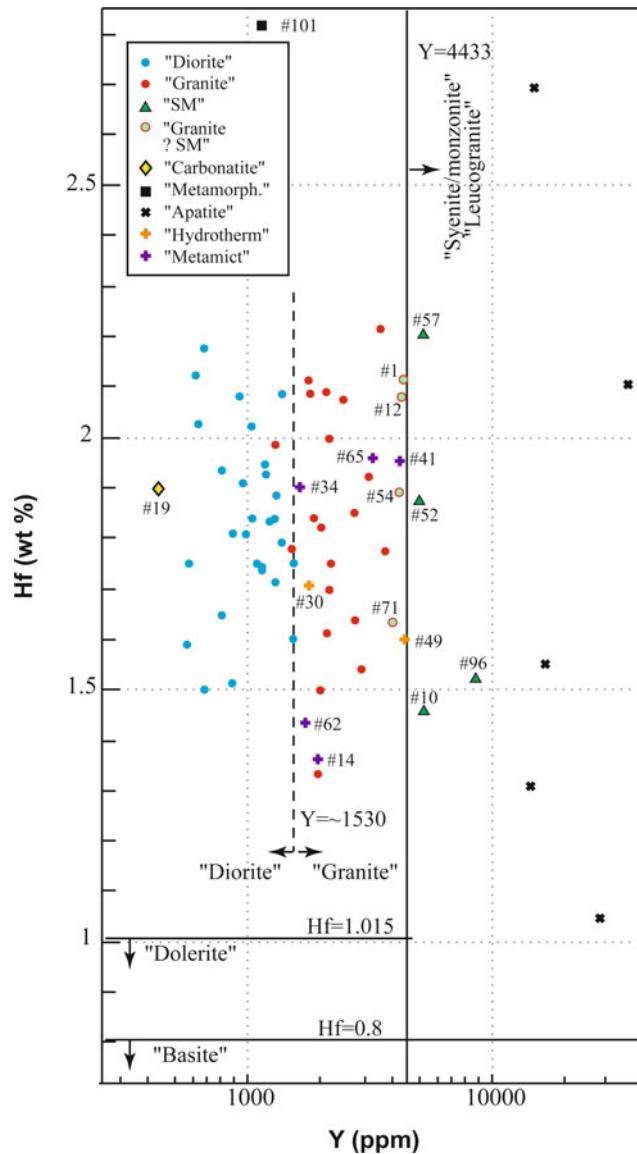


**Fig. 9** Classification diagrams of Hf and Y contents in detrital zircons from sample K12-006

2014, 2015, 2017; Khotylev and Tevelev 2017), which are oldest among these orogens and closest to the Southern Urals. Note that several data points fall directly into the field of isotopic parameters of the rocks of the southern Volga-Sarmatian collisional orogen (“VSO-field”). The age interval of the Paleoproterozoic dZr of 1.85–2.15 Ga fit well to a time interval of magmatic activity within the Volga-Sarmatian and Taratash orogens. The obtained data provide a very strong argument to consider the Volga-Sarmatian and Taratash orogens as the most probable source of Paleoproterozoic zircons in sample K12-006. However, it is needed to note that Hf isotopes of the Paleoproterozoic dZr from sample K12-006 have not recorded

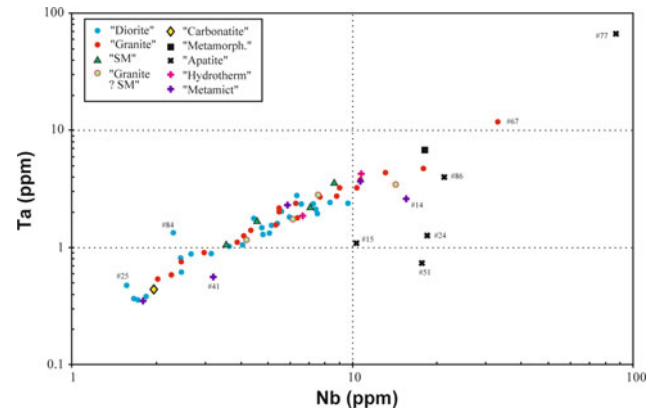


**Fig. 10** Classification diagrams of Ta and Nb contents in detrital zircons from sample K12-006

recycling of the Mesoarchean and older crust. This is difficult to explain because numerous dZr with signs of recycling of the Mesoarchean, Paleoproterozoic and even Hadean (single dZr) have been found in the Riphean strata of the Bashkir Uplift and they are considered as sourced from the Volga-Sarmatian and Taratash orogens (Fig. 14).

Numerous specific «carbonatite» zircons with ages of about 2.0, 2.5, 2.85 and 3.6 Ga were revealed in Riphean strata of the Bashkir Uplift (Fig. 14). However, in sample K12-006, only a single «carbonatite» zircon was found with an age of about ~2.7 Ga. Among the dZr from samples K12-006, numerous zircons with ages younger than 1.65 Ga have been found. These ages are absolutely atypical for the crystalline complexes of Volgo-Uralia. The primary sources of these dZr might be located either within the parts of the EEP that are situated very far from the Southern Urals, or outside the EEP, for example, in Kazakhstan. Erosional products of all these rocks might have been recycled in the Upper Ordovician Uraltau basin by well-developed long river systems.

For example, within Fennoscandia, the Mesoproterozoic rapakivi granites and paragenetically associated migmatites are widely developed (Sharkov 2010). The Sveconorwegian domain is composed mainly of the Mesoproterozoic (Danopolonian) and Early Neoproterozoic granite-metamorphic complexes (Bogdanova et al. 2008). The Volyn volcanic province in the southwestern part of Sarmatia composes of the Late Neoproterozoic (Ediacaran) basaltoids, volcanogenic-tuffogenic formations and felsic rocks (Shumlyansky et al. 2016b). Relicts of the Proto-Uralide-Timanide orogen, in the structure of which Late Neoproterozoic-Cambrian granitoids and metamorphites are widely represented (Kuznetsov et al. 2014a), are located in the northeastern margin of the EEP.

Small-volume crystalline complexes with ages <1.65 Ga are known in Western Urals, as well as in some of the Mesoproterozoic–Early Neoproterozoic (Riphean)

**Fig. 11** Diagram «U/Yb versus Hf» in dZr. Field “Continental survey”, arrows and inscriptions after (Grimes et al. 2015, Fig. 2)

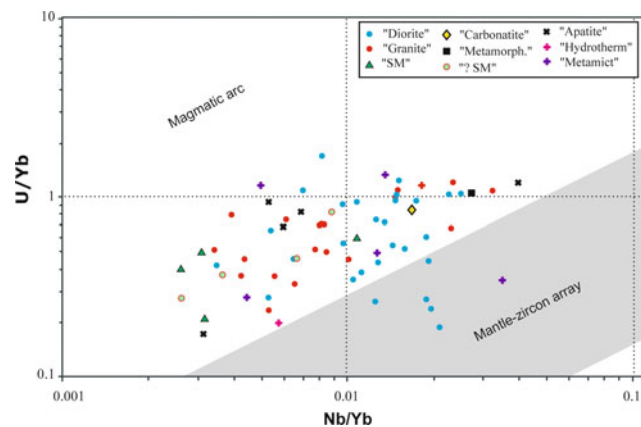
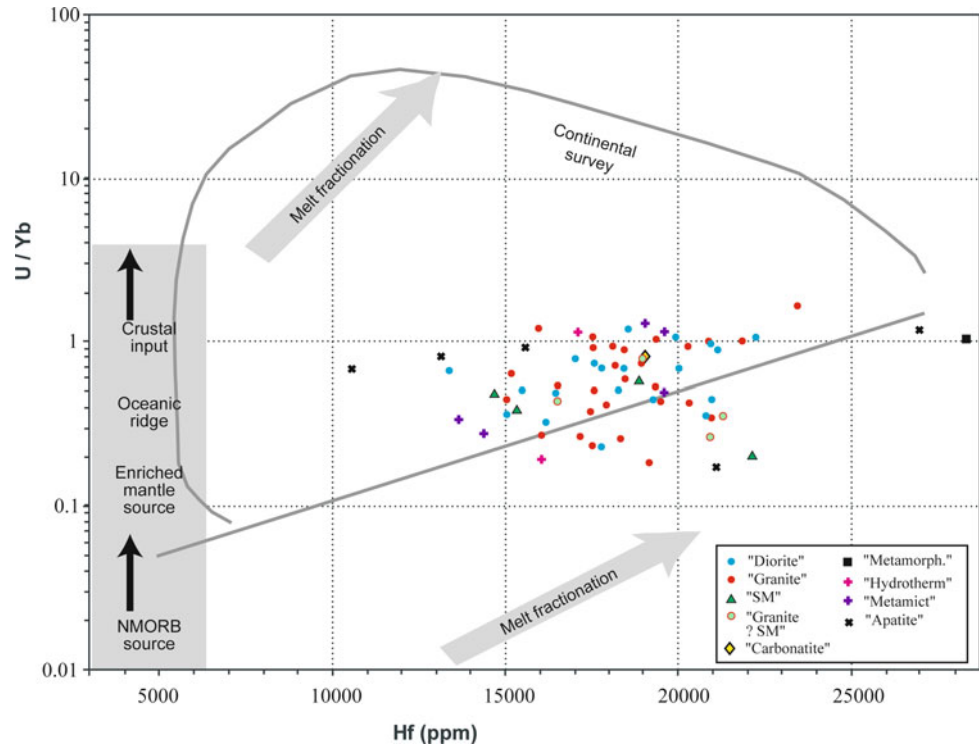


**Fig. 12** Diagram of the ratios “U/Yb versus Nb/Yb” in dZr. Fields “Magmatic arc” and “Mantle-zircon array” after (Grimes et al. 2015, Fig. 6c)

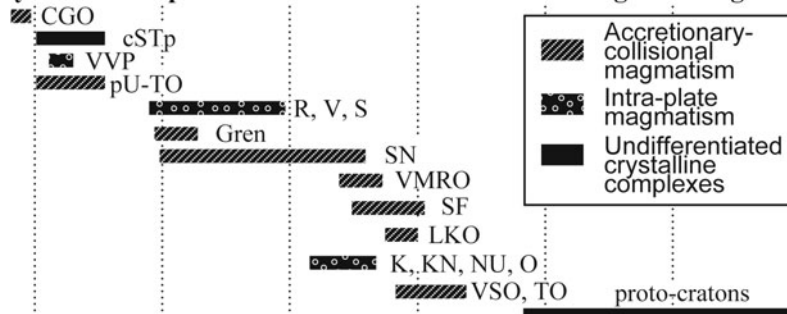
aulacogenes in the southeastern EEP (Gusikhin complex in the Pachelma aulacogene, etc.). However, ages that are available from those crystalline complexes form a very narrow time interval of 1.2–1.45 Ga and these complexes cannot be the only sources for numerous Mesoproterozoic 1.0–1.6 Ga dZr available in sample K12-006 (Fig. 13). Three ages of dZr from sample K12-006 coincide well with the age of intrusive rocks of the Berdyaush massif. However, their Hf isotope signatures differ considerably from those obtained for zircons from gabbro ( $\varepsilon_{\text{Hf}} = 4.6 \pm 1.0$ ) and from nepheline syenites, granite-rapakivi and quartz

syenite-diorites ( $\varepsilon_{\text{Hf}}$  of  $-5.3 \pm 0.7$ ,  $-6.0 \pm 0.9$  and  $-7.6 \pm 1.4$  respectively) (Ronkin et al. 2015a; b). Therefore, it is unlikely that the Berdyaush complex was a source of dZr in the K12-006 sample.

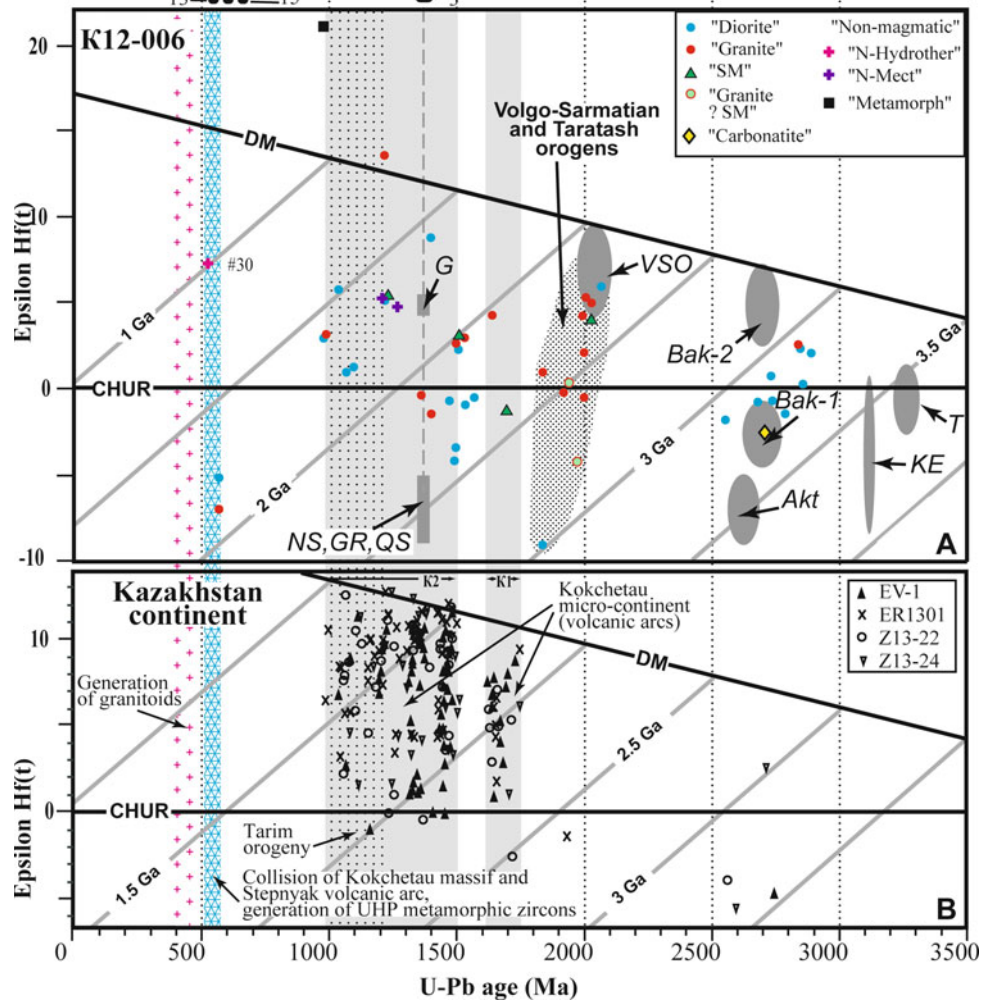
Other potential primary sources of the Mesoproterozoic zircons might have been crustal blocks, which form now the basement of the Scythian-Turanian plate or the Paleozooids of Central Kazakhstan (the basement of the Epi-Paleozoic Kazakhstan continent). A representative body of geochronological data has already been accumulated for the basement of the Epi-Paleozoic Kazakhstan continent, which allows us to reconstruct the main stages of the formation of its heterogeneous continental crust (Degtyarev et al. 2016, 2017). In accordance with these data (Fig. 13b), the basement of the Kokchetau microcontinent located in a core of the basement of the Epi-Paleozoic Kazakhstan continent is composed of juvenile material of Late Proterozoic and Mesoproterozoic intra-oceanic arcs. The earliest magmatic episode (K1) is dated at 1.85–1.65 Ga, the next episode (K2) lasted at least from 1.5 to 1.0 Ga. Its final phases occurred at 1.2–1.0 Ga and are known as the Tarim orogeny, relicts of which are preserved in Northern Kazakhstan (the North-Kazakhstan tectonic zone). The assembly of the Kazakhstan continent as a large heterogeneous crustal block and consolidation of its basement most likely took place during this orogeny.

The study of dZr from the Mesoproterozoic–Early Neoproterozoic (Riphean) cover of the Kokchetau Massif (4 samples) (Kovach et al. 2017) revealed several Archean dZr,

**Ages of crystalline complexes of the basement of EEP and neighbour regions**



**Ages of crystalline complexes of the Western Southern Urals**



◀ **Fig. 13** A comparison of «Diagrams  $\varepsilon_{\text{Hf}}$ » for detrital zircons from sample K12-006 from Upper Ordovician strata of the Uraltau Uplift (A) with «Diagrams  $\varepsilon_{\text{Hf}}$ » for detrital zircons from Riphean strata of Northern Kazakhstan (B), as well as with known ages of EEP basement and Western Urals complexes (upper part of the figure), which are possible sources of detrital zircons. A «Diagram  $\varepsilon_{\text{Hf}}$ » for dZr from sample K12-006. Grey oblique lines = lines of the Hf crustal model age of the protolith  $T_{\text{DM}}^{\text{C}}$ . Gray ellipses of the field of data points of ages and  $T_{\text{DM}}$ , estimated by the Sm-Nd isotopic system (complexes: T = Tashlyar, Akt = Aktanysh, Bak-1 and Bak-2—quartz diorites of Bakaly block) from (Bogdanova et al., 2010), for the southern part of the Volga-Sarmatian orogen (VSO-field) from (Bibikova et al. 2009), for Kolyvan enderbites (KE) from (Bogdanova et al. 2013). Gray rectangles are the fields of data points of ages and  $\varepsilon_{\text{Hf}}$  for rocks of the Berdyash complex of the Western Urals (G-gabbro, NS, GR, QS-nepheline syenites, granites rapakivi and quartz syeno-diorites, correspondently) from (Ronkin et al. 2015a; b). For other complexes of the Western Urals, the age intervals are shown only in the upper part of the figure. The dotted pattern shows the area correlated with the zircons generated by the Taratash and Volga-Sarmatian collisional orogen. B «Diagram  $\varepsilon_{\text{Hf}}$ » for dZr from Riphean Group sandstones of the Kokchetau Massif (samples EV1, ER1, Z13-22 and Z13-24) from (Kovach et al., 2017), which characterize the basement of the Kokchetau microcontinent. In the upper part of the figure, the bars show the age intervals for the EEP and Western Urals complexes. EEP: VSO, TO = complexes of the Volga-Sarmatian and Taratash orogens (Bibikova et al. 2009; Tevelev et al. 2014, 2015, 2017; Terentiev and Santosh 2016; Terentiev et al. 2016a, b, 2017, 2018; Khotylev and Tevelev 2017); K, KN, NU, O = plutons and rapakivi-like granites: Korosten, Korsun-Novomirgorod, Novo-Ukrainian, October plutons of the Ukraine Shield (Bogdanova et al. 2004; Shumlyanskyy et al., 2006, 2015, 2016a, 2017), granites of the Voronezh Crystalline Massif (Savko et al. 2014); LKO = complexes of the Lapland-Kola orogen, sutured Kola and Karelia proto-cratons (Lahtinen and Huhma 2019); SF = complexes of the Svecofennian domain (Kahkonen 2005); VMRO = complexes of the Volyn-Middle-Russian orogen, sutured Fennoscandia and Volgo-Sarmatia (Bogdanova et al. 2008); SN = complexes of the Sveco-Norwegian domain (Bingen et al. 2008a; b); Gren = complexes of the Sveconorwegian (Grenville) orogen, which sutured Proto-Baltica, Proto-Laurentia and Amazonia in the process of

assembling Rodinia; R, V, S = plutons and rapakivi-like granites: Riga, Vyborg and Salmi plutons (Bogdanova et al. 2008); pU-TO = complexes of the Proto-Uralide-Timanide orogen, which sutured Baltica and Arctica (Kuznetsov et al. 2009); VVP = complexes of the Volyn volcanic province (Shumlyanskyy et al., 2016b); cSTp = the basement of the Scythian-Turanian plate (Cadmides); CGO = Greenland Caledonian orogen, which sutured Arctic Europe and Laurentia. Western Urals: T = granitoids and metamorphites of the Taratash complex; 1—alkaline basaltoids of the Navysh complex (Ai Fm, Lower Riphean Burzyan Group, stratotypical location, Southern Urals)  $1752 \pm 18$  Ma (Krasnobaev et al. 2013a); 2—Saran gabbro-ultrabasic intrusive complex (Middle and Northern Urals), related to magma chambers of depleted mantle over a mantle plum,  $\sim 1750$  Ma (Petrov, 2017); 3—Berdyash intrusive massif  $1395 \pm 20$ ,  $1373 \pm 21$ ,  $1372 \pm 12$ ,  $1368.4 \pm 6.2$  and  $1369 \pm 13$  Ma (Puchkov 2010) (G—gabbro, NS—nepheline syenites, GR—granites-rapakivi, QS—quartz syeno-diorites); 4 and 5—granites of the Akhmerovo massif  $1413 \pm 45$  Ma (I-generation) and  $1381 \pm 23$  Ma (II-generation) (Krasnobaev et al., 2008); 6—intrusive rocks of the Kusa-Kopan and Ryabinov complexes (marking the northern side of the Zyuratkul fault), gabbro of the Kopan massif  $1385 \pm 25$  Ma, granites of Ryabinov  $1386 \pm 40$  Ma and Guben  $1330 \pm 16$ ,  $1330 \pm 27$  Ma massifs (Puchkov 2010); 7—bimodal volcanics of the Mashak Fm and its age analogous—Shatak and Kuvash Fms  $\sim 1385$  Ma (Puchkov, 2010); 8—volcanics of the Arsha Group  $-709.9 \pm 7.3$  Ma (Puchkov, 2010); 9—granitoids of the Barangulovo massif  $725 \pm 5$  Ma (Puchkov 2010); 10—metamorphic rocks (including HP and UHP rocks) of the Beloretsk block 600–550 Ma (Puchkov 2010); 11—rocks of the Mazara magmatic areal: granites  $681 \pm 14$ ,  $667 \pm 9.6$  Ma and gabbroids  $709 \pm 10$ ,  $704.2 \pm 8.3$  Ma (Kuznetsov 2009); 12—pyroxenites of the Kiryabin massif  $680 \pm 3.4$  Ma (Krasnobaev et al. 2013b); 13—trachybasalts and hyalophelinites of Dvoretz and granitoids of Europa complexes  $570 \div 550$  Ma (Petrov 2017); 14—weakly alkaline rocks of the Kusa complex and basalts of basal levels of the Tanin Fm 625–600 Ma (Maslov et al. 2013; Petrov 2017); 15—trachyandesites of the Shegra Fm, granosyenitic Troitsk and verlitic-gabbro-granodioritic Zhuravlik complexes  $680 \div 670$  Ma (Maslov et al. 2013; Petrov 2017); 16—tuffs layers of the Sylvitsa Group  $563.5 \pm 3.5$  (Kuznetsov et al. 2017c)

a small group of Late Proterozoic dZr (correlated with the **K1** episode) and a dominant population of the Mesoproterozoic zircons (correlated with the **K2** episode) (Fig. 13b). In the Late Neoproterozoic, the Kokchetau Massif collided with the Stepnyak volcanic arc, then the UHP complexes of a subduction zone were exhumed and became a source of specific metamorphic zircons with anomalously low Th/U ratios (Glorie et al. 2015). Later, extensive areas of the Kazakhstan continent were intruded by Paleozoic granitoids (Degtyarev et al. 2016, 2017).

Mesoproterozoic U-Pb ages and Hf isotope characteristics of dZr from sample K12-006 are well consistent with those from the Mesoproterozoic–Early Neoproterozoic (Riphean) cover of the Kokchetau Massif.

The only exception is that no 1.5–1.65 Ga dZr have been found in the Kokchetau Massif (a magmatic gap between **K1** and **K1** episodes), whereas several dZr with these ages have

been found in the K12-006 sample. The three youngest ages of dZr from the K12-006 sample agree well with the time of the collision between the Kokchetau Massif and the Stepnyak volcanic arc. The zircons with extremely low Th/U ratios sourced from the UHP complexes related to this event have been reported by Glorie et al. (2015). There have been no similar zircons found in the K12-006 sample. Note, however, that there has been revealed one «specific» dZr #30, classified as a zircon of «Hydrothermal» origin, which may be related to the same collisional event.

There are no geochronological data available on the deep-buried complexes of the basement of the Scythian-Turanian plate. This plate is interpreted as a belt of the Cadomian terranes, which extends from Europe along the southern margin of the EEP into the Central Asian Orogenic Belt as suggested by geophysical data and indirect correlations (Kuznetsov and Romanyuk 2021).

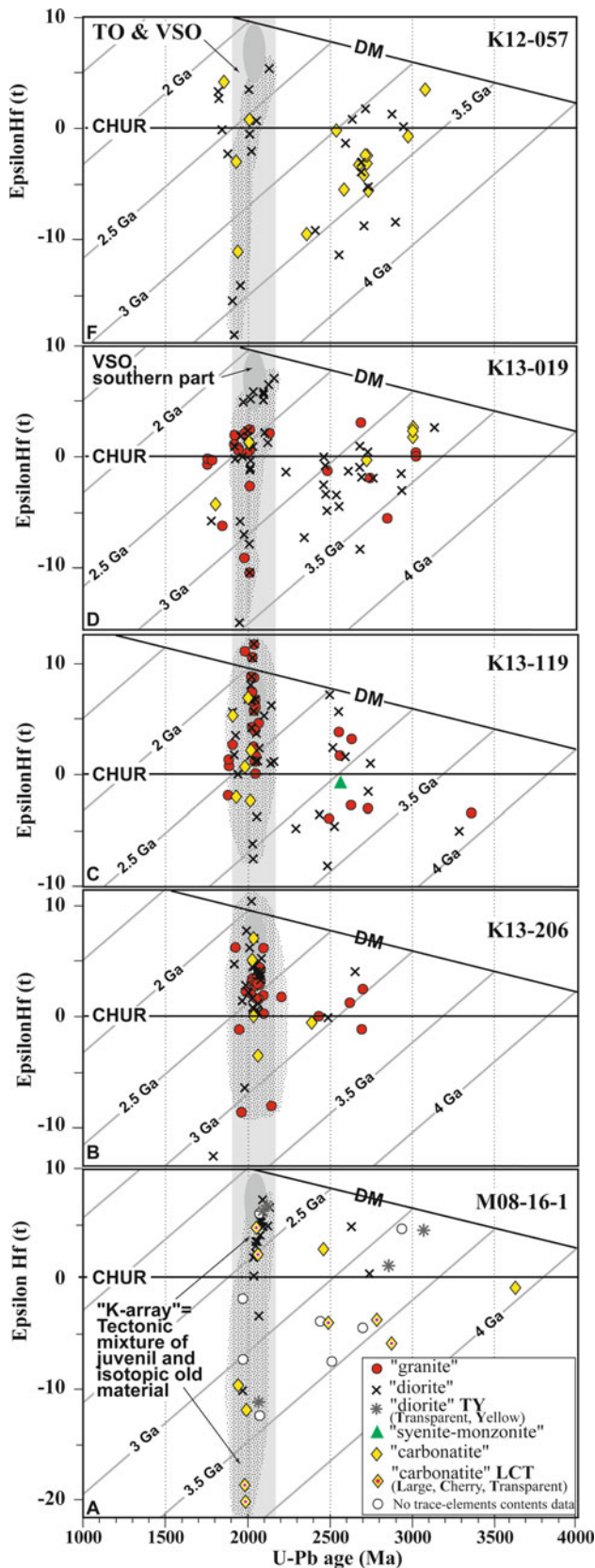


**Fig. 14** «Diagrams  $\epsilon_{\text{Hf}}$ » For detrital zircons from Riphean strata of the Bashkir Uplift. VSO and TO = the Volgo-Sarmatian and Taratash orogens. Sample locations see in Fig. 1. Data after Romanyuk et al. (2013, 2014, 2017, 2018, 2019a)

## 5 Conclusions

Integral characteristics of detrital zircons from Upper Ordovician sandstones of the Uraltau Uplift studied in the sample K12-006 show little similarities with U-Pb and Lu-Hf model ages of rocks, from the basement of Volga-Uralia (the southeastern part of the EEP) and with the same characteristics of detrital zircons from the Late Precambrian strata of the Bashkir Uplift and Kazakhstan. In contrast, the Mesoproterozoic detrital zircons from the sample K12-006 are well consistent with U-Pb ages and Hf isotope signatures of detrital zircons from the Mesoproterozoic–Early Neoproterozoic (Riphean) cover of the Kokchetau Massif. However, studied detrital zircons also revealed that they have alien relation to Volga-Uralia, Kazakhstan and the Western Urals and thus must have originated from other crustal blocks.

A very high similarity of the age spectra of dZr from Ordovician sandstones of the Uraltau and Bashkir Uplifts (samples K12-025 and K12-006, respectively; see Fig. 4a) allows concluding that the amalgamation of the Precambrian Bashkir and Uraltau basements occurred before Late Ordovician. Detritus of post-Upper Ordovician sedimentary complexes of the Bashkir and Uraltau Uplifts originated from identical feeding provinces and was deposited in the same basin, sealing its pre-Ordovician composite heterogeneous basement.

**Acknowledgements** We thank Vinod Singh for his help with preparing this publication and two anonymous reviewers for the valuable comments and recommendations, which improved the manuscript considerably. This study has been carried out by following the plans of the scientific research of the Geological Institute and Schmidt Institute of Physics of the Earth (both Institutes of Russian Academy of Science). The analytical data were obtained using instrumentation funded by DEST Systemic Infrastructure Grants, ARC LIEF, NCRIS/AuScope, industry partners and Macquarie University, and ARC FT110100685 grant support (Belousova EA). This is contribution 1568 from the ARC Centre of Excellence for Core to Crust Fluid Systems (<http://www.ccfs.mq.edu.au>) and 1432 in the GEMOC Key Centre (<http://www.gemoc.mq.edu.au>). Synthesis of materials and article preparation were supported by the grant of RF government № 075-15-2019-1883 (Orogenesis: Formation and Growth of Continents and Supercontinents).

## References

- Andersen T (2002) Correction of common lead in U-Pb analyses that do not report  $^{204}\text{Pb}$ . *Chem Geol* 192:59–79
- Belousova EA, Walters S, Griffin WL et al (2002) Igneous zircon: trace element compositions as indicators of source rock type. *Contrib Miner Petrol* 143(5):602–622
- Belousova EA, Griffin WL, O'Reilly SY (2006) Zircon crystal morphology, trace element signatures and Hf isotope composition as a tool for petrogenetic modeling: examples from eastern Australian granitoids. *J of Petrology* 47(2):329–353

- Belousova EA, Kostitsyn YA, Griffin WL et al (2010) The growth of the continental crust: constraints from zircon Hf-isotope data. *Lithos* 119(3–4):457–466
- Belousova EA, Gonzalez JM, Graham JJ et al (2015) The enigma of crustal zircons in upper-mantle rocks: clues from the Tumut ophiolite, southeast Australia. *Geology* 43(2):119–122
- Bibikova EV, Kimozova TI, Fugzan MM et al (2009) Sarmatia-Volgo-Uralia junction zone: isotopic-geochronologic characteristic of supracrustal rocks and granitoids. *Stratigr Geol Correl* 17(6):561–573
- Bingen B, Nordgulen O, Viola G (2008) A four-phase model for the Sveconorwegian orogeny, SW Scandinavia. *Norwegian J of Geology* 88:43–72
- Bingen B, Andersson J, Soderlund U et al (2008) The Mesoproterozoic in the Nordic countries. *Episodes* 31(1):29–34
- Black LP, Kamo SL, Allen CM et al (2004) Improved  $^{206}\text{Pb}/^{238}\text{U}$  microprobe geochronology by monitoring of a trace-element-related matrix effect: SHRIMP, ID-TIMS, ELA-ICP-MS and oxygen isotope documentation for a series of zircon standards. *Chem Geol* 205:115–140
- Bogdanova SV, Bingen B, Gorbatshev R et al (2008) The East European Craton (Baltica) before and during the assembly of Rodinia. *Precamb Res* 160:23–45
- Bogdanova SV, De Waele B, Bibikova EV et al (2010) Volgo-Uralia: the first U-Pb, Lu-Hf and Sm-Nd isotopic evidence of preserved Paleoproterozoic crust. *Am J Sci* 310:1345–1383
- Bogdanova SV, Belousova EA, De Waele B et al (2013) Zircon from Mesoarchean enderites of Volgo-Uralia: U-Pb age, REE Hf and O-isotope compositions. *Mineral Mag* 77(5):727
- Bogdanova SV, Pashkevich IK, Buryanov VB et al (2004) The 1.80–1.74-Ga gabbro-anorthosite-rapakivi Korosten Pluton in the Ukrainian Shield: a 3-D geophysical reconstruction of deep structure. *Tectonophysics* 381(1–4):5–27
- Bouvier A, Vervoort JD, Patchett PJ (2008) The Lu–Hf and Sm–Nd isotopic composition of CHUR: constraints from unequilibrated chondrites and implications for the bulk composition of terrestrial planets. *Earth Planet Sci Lett* 273:48–57
- Chapman JB, Gehrels GE, Ducea MN et al (2016) A new method for estimating parent rock trace element concentrations from zircon. *Chem Geol* 439:59–70
- Claoue-Long JC, King RW, Kerrich R (1990) Archean hydrothermal zircon in the Abitibi Greenstone Belt: constraints on the timing of gold mineralization—reply. *Earth Planet Sci Lett* 109:601–609. [https://doi.org/10.1016/0012-821X\(90\)90091-B](https://doi.org/10.1016/0012-821X(90)90091-B)
- Corfu F, Hanchar JM, Hoskin P-WO et al (2003) Atlas of zircon textures. *Rev Mineral Geochem* 53(1):469–500
- Corfu F, Davis DW (1991) Comment on “Archean hydrothermal zircon in the Abitibi greenstone belt: constraints on the timing of gold mineralization”. In: Claoue-Long JC, King RW, Kerrich R (eds). *Earth Planet Sci Lett* 104(2–4):545–552
- Degtyarev KE, Shatagin KN, Tret'yakov AA, (2016) Sources of Paleozoic granitic rocks and isotopic heterogeneity of the continental crust of the Aktau-Dzhungar microcontinent Central Kazakhstan. *Doklady Earth Sci* 470(2):1010–1013
- Degtyarev K, Yakubchuk A, Tret'yakov A et al (2017) Precambrian geology of the Kazakh uplands and Tien Shan: an overview. *Gondwana Res* 47:44–75
- Elhlou S, Belousova E, Griffin WL et al (2006) Trace element and isotopic composition of GJ-red zircon standard by laser ablation. *Geochimica Et Cosmochimica Acta* 70(18):158
- Fedotova AA, Bibikova EV, Simakin SG (2008) Ion-microprobe zircon geochemistry as an indicator of mineral genesis during geochronological studies. *Geochem Int* 46(9):912–927
- Ferry JM, Watson EB (2007) New thermodynamic models and revised calibrations for the Ti-in-zircon and Zr-in-rutile thermometers. *Contrib Miner Petrol* 154:429–437
- Fershtater GB, Krasnobaev AA, Bea F et al (2012) The geochemistry of zircon from the Urals igneous and metamorphic rocks. *Litosfera (lithosphere)* 4:13–29 (in Russian)
- Fornelli A, Langone A, Micheletti F et al (2014) The role of trace element partitioning between garnet, zircon and orthopyroxene on the interpretation of zircon U-Pb ages: an example from high-grade basement in Calabria (Southern Italy). *Int J Earth Sci* 103(2):487–507
- Fu B, Page FZ, Cavosie AJ et al (2008) Ti-in-zircon thermometry: applications and limitations. *Contrib Miner Petrol* 156:197–215
- Fu B, Mernagh TP, Kita NT et al (2009) Distinguishing magmatic zircon from hydrothermal zircon: a case study from the Gidginbung high-sulphidation Au–Ag–(Cu) deposit, SE Australia. *Chem Geol* 259:131–142
- Glorie S, Zhimulev FI, Buslov MM et al (2015) Formation of the Kokchetau subduction–collision zone (northern Kazakhstan): insights from zircon. *Gondwana Res* 27:424–438
- Golionko BG, Artemova OA (2016) Late Precambrian and Paleozoic deformations of the eastern part of the Bashkir anticlinorium (Southern Urals). *MOIP Bull Serie Geol* 91(6):3–10 (in Russian)
- Griffin WL, Pearson NJ, Belousova EA et al (2000) The Hf isotope composition of cratonic mantle: LAM-MC-ICPMS analysis of zircon megacrysts in kimberlites. *Geochim Cosmochim Acta* 64:133–147
- Griffin WL, Wang X, Jackson SE et al (2002) Zircon chemistry and magma genesis, SE China: in-situ analysis of Hf isotopes, Pingtan and Tonglu igneous complexes. *Lithos* 61:237–269
- Griffin WL, Belousova EA, Shee SR et al (2004) Archean crustal evolution in the northern Yilgarn Craton: U-Pb and Hf-isotope evidence from detrital zircons. *Precamb Res* 131:231–282
- Griffin WL, Belousova EA, Walters SG et al (2006) Archean and Proterozoic crustal evolution in the Eastern Succession of the Mt Isa district, Australia: U-Pb and Hf-isotope studies of detrital zircons. *Aust J Earth Sci* 53:125–149
- Griffin WL, Belousova EA, O'Reilly SY (2007) TerraneChron analysis of zircons from Western Australian samples record. *Geol Surv West Aust* 4:1–52
- Griffin WL, Powell WJ, Pearson NJ et al (2008) GLITTER: data reduction software for laser ablation ICP-MS / Ed. P.J. Sylvester. *Laser ablation ICP-MS in the Earth sciences: current practices and outstanding issues. Mineral Assoc Canada Short Course* 40:308–311
- Grimes CB, John BE, Kelemen PB et al (2007) Trace element chemistry of zircons from oceanic crust: a method for distinguishing detrital zircon provenance. *Geology* 35:643–646
- Grimes CB, Wooden JL, Cheadle MJ et al (2015) “Fingerprinting” tectono-magmatic provenance using trace elements in igneous zircon. *Contrib Mineral Petrol* 170(5–6):Article 46
- Harrison TM, Watson EB, Aikman AB (2007) Temperature spectra of zircon crystallization in plutonic rocks. *Geology* 35(7):635–638
- Hawkesworth CJ, Kemp AIS (2006) Using hafnium and oxygen isotopes in zircons to unravel the record of crustal evolution. *Chem Geol* 226:144–162
- Heaman LM, Bowins R, Crocket J (1990) The chemical composition of igneous zircon suites: implications for geochemical tracer studies. *Geochim Cosmochim Acta* 54(6):1597–1607
- Horstwood MSA, Kosler J, Gehrels G et al (2016) Community-derived standards for LA-ICP-MS U-(Th)-Pb geochronology—uncertainty propagation, age interpretation and data reporting. *Geostand Geoanal Res* 40(3):311–332

- Hoskin PWO (2005) Trace-element composition of hydrothermal zircon and the alteration of Hadean zircon from the Jack Hills, Australia. *Geochim Cosmochim Acta* 69:637–648
- Hoskin PO, Ireland TR (2000) Rare earth element chemistry of zircon and its use as a provenance indicator. *Geology* 28(7):627–630
- Hoskin PWO, Kinny PD, Wyborn D et al (2000) Identifying accessory mineral saturation during differentiation in granitoid magmas: an integrated approach. *J Petrol* 41:1365–1396
- Hoskin PWO, Schaltegger U (2003) The composition of zircon and igneous and metamorphic petrogenesis. In: Hancher JM, Hoskin PWO (Eds) *Zircon. Rev Mineral Geochem* 53:27–62
- Hu FF, Fan HR, Yang JH et al (2004) Mineralizing age of the Rushan lode gold deposit in the Jiaodong Peninsula: SHRIMP U-Pb dating on hydrothermal zircon. *Chin Sci Bull* 49:1629–1636
- Ivanov KS (1998) Main Features of Geological History (1.6–0.2 Ga) and Structure of the Urals. Nauka, Yekaterinburg (in Russian)
- Jackson SE, Pearson NJ, Griffin WL et al (2004) The application of laser ablation-inductively coupled plasma-mass spectrometry to in situ U-Pb zircon geochronology. *Chem Geol* 211:47–69
- Kaczmarek MA, Müntener O, Rubatto D (2008) Trace element chemistry and U-Pb dating of zircons from oceanic gabbros and their relationship with whole rock composition (Lanzo, Italian Alps). *Contrib Miner Petrol* 155(3):295–312
- Kostitsyn YA, Belousova EA, Silant'ev SA, Bortnikov NS, Anosova MO (2015) Modern problems of geochemical and U-Pb geochronological studies of zircon in oceanic rocks. *Geochem Int* 53:759–785. <https://doi.org/10.1134/S0016702915090025>
- Kahkonen Y (2005) Svecofennian supracrustal rocks. In: Lehtinen M, Nurmi JA, Ramo OT (eds) *Precambrian geology of Finland—key to the evolution of the Fennoscandian shield*. Elsevier B.V, Amsterdam, pp 343–406
- Kebede T, Horie K, Hidaka H et al (2007) Zircon ‘microvein’ in peralkaline granitic gneiss, western Ethiopia: origin, SHRIMP U-Pb geochronology and trace element investigations. *Chem Geol* 242:76–102
- Kerrick R, King R (1993) Hydrothermal zircon and baddeleyite in Val-Dor Archean mesothermal gold deposits: characteristics, compositions, and fluid-inclusion properties, with implications for timing of primary gold mineralization. *Can J Earth Sci* 30:2334–2351
- Khotylev AO, Tevelev AV (2017) Geochemical characteristics of the early Riphean Navysh volcanic complex (Southern Urals). *Mosc Univ Geol Bull* 73(1):24–30
- Kirkland CL, Smithies RH, Taylor RJM et al (2015) Zircon Th/U ratios in magmatic environments. *Lithos* 212–215:397–414
- Kovach V, Kotov A, Tolmacheva E, Degtyarev K, Tretyakov A, Wang K-L, Chung S-L, Lee H-Y, Jahn B-M (2017) Sources and provenance of the Neoproterozoic placer deposits of the Northern Kazakhstan: Implication for continental growth of the western Central Asian Orogenic Belt. *Gondwana Res* 47:28–43
- Krasnobaev AA, Puchkov VN, Kozlov VI et al (2008) The Akhmerovo granite massif: a proxy of Mesoproterozoic intrusive magmatism in the Southern Urals. *Dokl Earth Sci* 418(1):103–108
- Krasnobaev AA, Puchkov VN, Sergeeva ND et al (2013) Zirconology of pyroxenites from the Kiryabinka pyroxenite-gabbro complex (Southern Urals). *Dokl Earth Sci* 450(1):531–535
- Krasnobaev AA, Puchkov VN, Kozlov VI et al (2013) Zirconology of Navysh volcanic rocks of the Ai Suite and the problem of the age of the Lower Riphean boundary in the Southern Urals. *Dokl Earth Sci* 448(2):185–190
- Kuznetsov NB, Romanyuk TV (2021) Peri-Gondwanan Blocks in the Structure of the Southern and Southeastern Framing of the East European Platform. *Geotectonics* 55:439–472. <https://doi.org/10.1134/S0016852121040105>
- Kuznetsov NB, Shazillo AV (2011) The first finds of skeletal fossils in the Kuk-Karauk Formation of the Asha Group (Southern Urals) and their significance for determining the beginning of the Pre-Uralian-Timianian orogeny. *Dokl Earth Sci* 440(1):1239–1244
- Kuznetsov NB, Romanyuk TV, Shatsillo AV et al (2012) The first results of the bulk U/Pb-dating of detrital zircons (LA-ICP-MS) from Asha Formation, the Southern Urals—the stratigraphic, paleogeographic and paleo-tectonic aspects. *Dokl Earth Sci* 447(1):1240–1246
- Kuznetsov NB, Maslov AV, Belousova EA et al (2013) The first U-Pb (LA-ICP-MS) isotope data of detrital zircons from the basal levels of the Riphean Stratotype. *Dokl Earth Sci* 451(1):724–728
- Kuznetsov NB, Meert JG, Romanyuk TV (2014) Ages of the detrital zircons (U/Pb, LA-ICP-MS) from latest Neoproterozoic—Middle Cambrian(?) Asha group and early Devonian Takaty formation, the south-western Urals: a testing of an Australia-Baltica connection within the Rodinia. *Precambr Res* 244:288–305
- Kuznetsov NB, Romanyuk TV, Shatsillo AV et al (2014) The first results of the U/Pb-dating (LA-ICP-MS) of the detrital zircons from sandstones of the Upper Emsian Takata Formation, the Western Urals (with a problem of an ultimate source of the Uralian diamond placers). *Dokl Earth Sci* 455(2):370–375
- Kuznetsov NB, Belousova EA, Degtyarev KE et al (2016) The first results of the U/Pb dating of detrital zircons from the later Ordovician sandstones of the Bashkir uplifts (the Southern Urals). *Dokl Earth Sci* 467(2):325–330
- Kuznetsov NB, Belousova EA, Romanyuk TV et al (2017) The first results of U/Pb dating detrital zircons from sandstones of Zigalga Formation (Middle Riphean, the South Urals). *Dokl Earth Sci* 475(2):862–866
- Kuznetsov NB, Gorozhanin VM, Belousova EA et al (2017) The first results of U/Pb dating of detrital zircons from Ordovician terrigenous sequences of Sol-Iletsk arch of the East-European Platform. *Dokl Earth Sci* 473(2):381–385
- Kuznetsov NB, Belousova EA, Krupenin MT et al (2017) The results of geochronological and isotope-geochemical study of zircon from tuffs Sylvitsa Group (Western slope of the Middle Urals): the origin of ash layers in Vendian strata of the East European platform. *Dokl Earth Sci* 473(1):360–363
- Kuznetsov NB, Belousova EA, Romanyuk TV (2018) Geochemical and Lu-Hf isotope (LA-ICP-MS) systematic of detrital zircons from the Ordovician sandstones of the Sol-Iletsk arch (Russia, Northern Caspian, borehole Ordovician-2). *Archaeol Anthropol* 3(1):31–58
- Kuznetsov NB, Belousova EA, Griffin WL et al (2019) Pre-mesozoic Crimea as a continuation of the Dobrogea platform: insights from detrital zircons in upper Jurassic conglomerates Mountainous Crimea. *Int J Earth Sci* 108(7):2407–2428
- Kuznetsov NB (2009) Protouralide-Timianide complexes and Late Cambrian-Early Paleozoic evolution of eastern and north-eastern margins of East-European platform (Doctoral thesis). Geological Institute RAS, Moscow (in Russian). <https://www.dlib.rsl.ru/viewer/01003464837#?page=1>
- Lahtinen R, Huhma H (2019) A revised geodynamic model for the Lapland-Kola Orogen. *Precambr Res* 330:1–19
- Linnemann U, Ouzegane K, Drareni A et al (2011) Sands of West Gondwana: an archive of secular magmatism and plate interactions—a case study from the Cambro-Ordovician section of the Tassili Ouan Ahaggar (Algerian Sahara) using U-Pb-LA-ICP-MS detrital zircon ages. *Lithos* 123:188–203
- Liu F-L, Xu Z-Q (2004) Fluid inclusions hidden in coesite-bearing zircons in ultrahigh-pressure metamorphic rocks from southwestern Sulu terrane in eastern China. *Chin Sci Bull* 49:396–404
- Liu J-B, Ye K, Maruyama S, Cong B, Fan H (2001) Mineral inclusions in zircon from gneisses in the ultrahigh-pressure zone of the Dabie Mountains, China. *J Geol* 109:523–535

- Liu J, Liu F, Ding Z et al (2013) U-Pb dating and Hf isotope study of detrital zircons from the Zhifu Group, Jiaobei Terrane, North China Craton: provenance and implications for Precambrian crustal growth and recycling. *Precambr Res* 235:230–250
- Ludwig KR (2012) User's manual for Isoplot 3.75. A geochronological toolkit for Microsoft Excel. Berkeley Geochronology Center. Spec. Publ, No 5. 75 p
- Maslov AV, Meert J, Levashova NM et al (2013) New data about age of the Vendian glacial deposits (Middle Urals). *Dokl Earth Sci* 449 (1):303–308
- Maslov AV (2004) Riphean and Vendian sedimentary sequences of the Timanides and Uralides, the eastern periphery of the East European Craton. In: The Neoproterozoic Timanide Orogen of Eastern Baltica. Gee DG, Pease V (Eds). Geological Society of London, Memoirs. 30:19–35
- McDonough WF, Sun SS (1995) The composition of the Earth. *Chem Geol* 120:223–253
- Pelleter E, Cheilletz A, Gasquet D et al (2007) Hydrothermal zircons: a tool for ion microprobe U-Pb dating of gold mineralization (Tamlalt-Menhouhou gold deposit—Morocco). *Chem Geol* 245:135–161
- Petrov GA (2017) Geology of the Pre-Palaeozoic complexes in the middle part of the Uralian mobile belt. (Doctoral thesis). Geological Institute RAS, S-Petersburg. University (in Russian). <https://www.docplayer.ru/45643414-Petrov-georg-askoldovich-geologiya-dopaleozoyskih-kompleksov-sredney-chasti-uralskogo-podvizhnogo-poyasa.html>
- Pettke T, Audetat A, Schaltegger U et al (2005) Magmatic-to-hydrothermal crystallization in the W-Sn mineralized Mole Granite (NSW, Australia)—Part II: evolving zircon and thorite trace element chemistry. *Chem Geol* 220:191–213
- Puchkov VN (2010) Geology of the Urals and Cis-Urals (actual problems of stratigraphy, tectonics, geodynamics and metallogeny). Design Poligraph Service, Ufa, 280 p (in Russian)
- Ramezani J, Dunning GR, Wilson MR (2000) Geologic setting, geochemistry of alteration, and U-Pb age of hydrothermal zircon from the Silurian Stog'er Tight gold prospect, Newfoundland Appalachians, Canada. *Explor Min Geol* 9:171–188
- Romanyuk TV, Kuznetsov NB, Maslov AV et al (2014) Geochemical and Lu/Hf Isotopic (LA-ICP-MS) signature of detrital zircons from sandstones of the basal levels of the Riphean stratotype. *Dokl Earth Sci* 459(1):1356–1360
- Romanyuk TV, Kuznetsov NB, Belousova EA et al (2017) Geochemical and Lu/Hf-isotopic (LA-ICP-MS) systematics of detrital zircons from the Upper Ordovician sandstones of the Bashkir uplift (Southern Urals). *Dokl Earth Sci* 472(2):134–137
- Romanyuk TV, Kuznetsov NB, Belousova EA et al (2018) Paleotectonic and paleo-geographic conditions for the accumulation of the lower Riphean Ai Formation in the Bashkir uplift (Southern Urals): the Terrane Chrono® detrital zircon study. *Geodyn Tectonophys* 9 (1):1–37
- Romanyuk TV, Kuznetsov NB, Maslov AV et al (2013) Geochemical and Lu/Hf (LA-ICP-MS) systematics of detrital zircons from Upper Riphean Lemeza Fm., Southern Urals. *Dokl Earth Sci* 453(2):1200–1204
- Romanyuk TV, Belousova EA, Kuznetsov NB et al (2019a) A search for sources of the detritus of Ordovician sandstones from the Sol-Iletsk block (Ordovician-2 borehole) based on the first data of the geochemical and Lu/Hf isotopic systematics of zircons. *Doklady Earth Sci* 487(1):795–799. <https://doi.org/10.1134/S1028334X19070067>
- Romanyuk TV, Kuznetsov NB, Puchkov VN et al (2019b) Local source of detritus for rocks of the Ai Formation (basal level of the Lower Riphean stratotype, the Bashkir Uplift, Southern Urals): evidence from U-Pb (LA-ICP-MS) dating of detrital zircons. *Doklady Earth Sci* 484(1):53–57. <https://doi.org/10.1134/S1028334X19010069>
- Romanyuk TV, Kuznetsov NB, Puchkov VN et al (2000) Age and Stratigraphic Position of Sedimentary Sequences of the Bagrush Mountains (Southern Urals) Based on the Results of U–Pb Dating (LA–ICP–MS) of Detrital Zircons. *Doklady Earth Sciences* 493:593–599 <https://doi.org/10.1134/S1028334X20080188>
- Ronkin YuL, Maslov AV, Gerdes A (2015) REE and Lu-Hf systematics of zircons from rapakivi granites and associated rocks of supercontinent Nuna (Columbia). *Dokl Earth Sci* 461(1):277–282
- Ronkin YuL, Gerdes A, Nesbit R (2015) Zircon of the granites rapakivi and associating rocks of the Southern Urals: REE and Lu-Hf isotopic constraints. *Proc Inst Geol Geochem Ural Branch Russ Acad Sci* 162:222–228 (in Russian)
- Rubatto D (2002) Zircon trace element geochemistry: partitioning with garnet and the link between U-Pb ages and metamorphism. *Chem Geol* 184(1–2):123–138
- Rubatto D (2017) Zircon: the Metamorphic Mineral. *Rev Mineral Geochem* 83(1):261–295
- Rubatto D, Hermann J (2007) Experimental zircon/melt and zircon/garnet trace element partitioning and implication for the geochronology of crustal rocks. *Chem Geol* 241(1–2):38–61
- Rubin JN, Henry CD, Price JG (1989) Hydrothermal zircons and zircon overgrowths, Sierra-Blanca Peaks, Texas. *Am Miner* 74:865–869
- Rubin JN, Henry CD, Price JG (1993) The mobility of zirconium and other “immobile” elements during hydrothermal alteration. *Chem Geol* 110(1–3):29–47
- Savko KA, Samsonov AV, Larionov AN et al (2014) Paleo-Proterozoic A and S-granites in the eastern Voronezh crystalline massif: geochronology, petrogenesis, and tectonic setting of origin. *Petrology* 22(3):205–233
- Schaltegger U, Pettke T, Audétat A et al (2005) Magmatic-to-hydrothermal crystallization in the W-Sn mineralized mole granite (NSW, Australia)—Part I: crystallization of zircon and REE-phosphates over three million years—a geochemical and U–Pb geochronological study. *Chem Geol* 220:215–235
- Schaltegger U (2003) The composition of zircon and igneous and metamorphic petrogenesis. In: Hanchar JM, Hoskin PWO (eds) *Zircon, Reviews in Mineralogy and Geochemistry*, 53, pp 27–62. Mineralogical Society of America
- Scherer E, Münker C, Mezger K (2001) Calibration of the Lu-Hf clock. *Science* 293:683–687
- Schulz B, Klemd R, Braetz H (2006) Host rock compositional controls on zircon trace element signatures in metabasites from the Austroalpine basement. *Geochim Cosmochim Acta* 70:697–710
- Sharkov EV (2010) Middle-proterozoic anorthosite–rapakivi granite complexes: an example of within-plate magmatism in abnormally thick crust: evidence from the East European Craton. *Precambr Res* 183(4):689–700
- Shumlyanskyy L, Ellam RM, Mitrokhin O (2006) The origin of basic rocks of the Korosten AMCG complex, Ukrainian shield: implication of Nd and Sr isotope data. *Lithos* 90(3–4):214–222
- Shumlyanskyy L, Ernst R, Billstrom K (2015) A U-Pb Baddeleyite age of the Davydky gabbro-syenite massif of the Korosten plutonic complex. *Geochem Ore Form* 35:37–42
- Shumlyanskyy L, Nosova A, Billstrom K et al (2016) The U-Pb zircon and baddeleyite ages of the Neoproterozoic Volyn Large Igneous Province: implication for the age of the magmatism and the nature of a crustal contaminant. *GFF* 138(1):1–14
- Shumlyanskyy L, Hawkesworth C, Billström K et al (2017) The origin of the Palaeoproterozoic AMCG complexes in the Ukrainian shield: new U-Pb ages and Hf isotopes in zircon. *Precambr Res* 292:216–239

- Shumlyanskyy L, Mitrokhin O, Billstrom K et al (2016a) The ca. 1.8 Ga mantle plume related magmatism of the central part of the Ukrainian shield. *GFF* 138(1):86–101
- Sindern S, Hetzel R, Schulte BA et al (2005) Proterozoic magmatic and tectonometamorphic evolution of the Taratash complex, Central Urals, Russia. *Earth and environmental science. Int J Earth Sci* 94 (3):319–335
- Skublov SG, Berezin AV, Berezhnaya NG (2012) General relations in the trace-element composition of zircons from eclogites with implications for the age of eclogites in the Belomorian mobile belt. *Petrology* 20(5):427–449
- Stratotype of Riphean. *Stratigraphy. Geochronology* (1983) Nauka, Moscow (in Russian)
- Teipel U, Eichhorn R, Loth G et al (2004) A U-Pb SHRIMP and Nd isotopic data from the western Bohemian Massif (Bayerischer Wald, Germany): implications for Upper Vendian and Lower Ordovician magmatism. *Int J Earth Sci (geol Rundsch)* 93:782–801
- Terentiev RA, Santosh M (2016) Detrital zircon geochronology and geochemistry of metasediments from the Vorontsovka terrane: implications for microcontinent tectonics. *Int Geol Rev* 58 (9):1108–1126
- Terentiev RA, Skryabin VY, Santosh M (2016) U-Pb zircon geochronology and geochemistry of Paleoproterozoic magmatic suite from East Sarmatian Orogen: tectonic implications on Columbia supercontinent. *Precambr Res* 273:165–184
- Terentiev RA, Savko KA, Santosh M (2016) Paleoproterozoic crustal evolution in the East Sarmatian Orogen: petrology, geochemistry, Sr–Nd isotopes and zircon U-Pb geochronology of andesites from the Voronezh Massif, Western Russia. *Lithos* 246–247:61–80
- Terentiev RA, Savko KA, Santosh M (2017) Paleoproterozoic evolution of the back-arc-arc system in the East Sarmatian orogen (East European craton): zircon SHRIMP Geochronology & geochemistry of the Losevo volcanic suite. *Am J Sci* 317(5):707–753
- Terentiev RA, Savko KA, Santosh M (2018) Post-collisional two-stage magmatism in the East Sarmatian orogen, East European craton: evidence from the Olkhovsky ring complex. *J Geol Soc* 175(1):86–99
- Tevelev AV, Kosheleva IA, Khotylev AO et al (2014) Peculiarities of the structure and evolution of the Riphean Ai volcanic complex South Urals. *Mosc Univ Geol Bull* 69(5):289–298
- Tevelev AV, Kosheleva IA, Tevelev AV et al (2015) New data on the isotope ages of the Taratash and Aleksandrovka metamorphic complexes. *Mosc Univ Geol Bull* 70(1):24–40
- Tevelev AV, Mosejchuk VM, Tevelev AV et al (2017) The zircon-age distribution in metamorphic rocks of the Taratash block, Southern Urals (an initial provenance signal). *Mosc Univ Geol Bull* 72 (5):314–319
- Veevers JJ, Saeed A, Belousova EA et al (2005) U-Pb ages and source composition by Hf-isotope and trace-element analysis of detrital zircons in Permian sandstone and modern sand from southwestern Australia and a review of the paleogeographical and denudational history of the Yilgarn Craton. *Earth Sci Rev* 68:245–279
- Veevers JJ, Belousova EA, Saeed A et al (2006) Pan-Gondwanaland detrital zircons from Australia analysed for Hf-isotopes and trace elements reflect an ice-covered Antarctic provenance of 700–500 Ma age, TDM of 2.0–1.0 Ga, and alkaline affinity. *Earth Sci Rev* 76:135–174
- Vermeesch P (2012) On the visualisation of detrital age distributions. *Chem Geol* 312–313:190–194
- Vermeesch P (2018) IsoplotR: a free and open toolbox for geochronology. *Geosci Front* 9:1479–1493
- Wanless VD, Perfit MR, Ridley WI et al (2011) Volatile abundances and oxygen isotopes in basaltic to dacitic lavas on mid-ocean ridges: the role of assimilation at spreading centers. *Chem Geol* 287:54–65
- Watson EB, Wark DA, Thomas JB (2006) Crystallization thermometers for zircon and rutile. *Contrib Miner Petrol* 151:413–433
- Wiedenbeck M, Alle P, Corfu F et al (1995) Three natural zircon standards for U-Th-Pb, Lu-Hf, trace-element and REE analyses. *Geostand Newsl* 19:1–23
- Wiedenbeck M, Hanchar JM, Peck WH et al (2004) Further characterization of the 91500 zircon crystal. *Geostand Geoanal Res* 28:9–39
- Yuan H-L, Gao S, Dai M-N et al (2008) Simultaneous determinations of U-Pb age, Hf isotopes and trace element compositions of zircon by excimer laser-ablation quadrupole and multiple-collector ICP-MS. *Chem Geol* 247:100–118
- Zhang Z-M, Shen K, Wang JL et al (2009) Petrological and geochronological constraints on the formation, subduction and exhumation of the continental crust in the southern Sulu orogen, eastern-central China. *Tectonophysics* 475(2):291–307
- Zhang Sh, Li Z-X, Evans DAD et al (2012) Pre-Rodinia supercontinent Nuna shaping up: a global synthesis with new paleomagnetic results from North China. *Earth Planet Sci Lett* 353–354:145–155